1   **A comprehensive quantification of global nitrous oxide sources and sinks**

2

3   Hanqin Tian[1], Rongting Xu[1], Josep G. Canadell[2], Rona L. Thompson[3], Wilfried Winiwarter[4,5],
4   Parvadha Suntharalingam[6], Eric A. Davidson[7], Philippe Ciais[8], Robert B. Jackson[9,10,11], Greet
5   Janssens-Maenhout[12,13], Michael J. Prather[14], Pierre Regnier[15], Naiqing Pan[1,16], Shufen Pan[1],
6   Glen P. Peters[17], Hao Shi[1], Francesco N. Tubiello[18], Sönke Zaehle[19], Feng Zhou[20], Almut
7   Arneth[21], Gianna Battaglia[22], Sarah Berthet[23], Laurent Bopp[24], Alexander F. Bouwman[25,26,27],
8   Erik T. Buitenhuis[6,28], Jinfeng Chang[8,29], Martyn P. Chipperfield[30,31], Shree R. S. Dangal[32],
9   Edward Dlugokencky[33], James W. Elkins[33], Bradley D. Eyre[34], Bojie Fu[16,35], Bradley Hall[33],
10   Akihiko Ito[36], Fortunat Joos[22], Paul B. Krummel[37], Angela Landolfi[38,39], Goulven G. Laruelle[15],
11   Ronny Lauerwald[8,15,40], Wei Li[8,41], Sebastian Lienert[22], Taylor Maavara[42], Michael MacLeod[43],
12   Dylan B. Millet[44], Stefan Olin[45], Prabir K. Patra[46,47], Ronald G. Prinn[48], Peter A. Raymond[42],
13   Daniel J. Ruiz[14], Guido R. van der Werf[49], Nicolas Vuichard[8], Junjie Wang[27], Ray F. Weiss[50],
14   Kelley C. Wells[44], Chris Wilson[30,31], Jia Yang[51] & Yuanzhi Yao[1]

15

16   [1]International Center for Climate and Global Change Research, School of Forestry and Wildlife
17   Sciences, Auburn University, Auburn, AL, USA
18   [2]Global Carbon Project, CSIRO Oceans and Atmosphere, Canberra, Australian Capital Territory,
19   Australia
20   [3]Norsk Institutt for Luftforskning, NILU, Kjeller, Norway
21   [4]International Institute for Applied Systems Analysis, Laxenburg, Austria
22   [5] Institute of Environmental Engineering, University of Zielona Góra, Zielona Góra, Poland.
23   [6]School of Environmental Sciences, University of East Anglia, Norwich, UK
24   [7]Appalachian Laboratory, University of Maryland Center for Environmental Science, Frostburg,
25   MD, USA
26   [8]Laboratoire des Sciences du Climat et de l'Environnement, LSCE, CEA CNRS, UVSQ
27   UPSACLAY, Gif sur Yvette, France
28   [9]Department of Earth System Science, Stanford University, Stanford, CA, USA
29   [10]Woods Institute for the Environment, Stanford University, Stanford, CA, USA
30   [11]Precourt Institute for Energy, Stanford University, Stanford, CA, USA
31   [12]European Commission, Joint Research Centre (JRC), Ispra, Italy
32   [13]Ghent University, Faculty of Engineering and Architecture, Ghent, Belgium
33   [14]Department of Earth System Science, University of California Irvine, Irvine, CA, USA
34   [15]Department Geoscience, Environment & Society, Université Libre de Bruxelles, Brussels,
35   Belgium
36   [16]State Key Laboratory of Urban and Regional Ecology, Research Center for Eco-Environmental
37   Sciences, Chinese Academy of Sciences, Beijing, China
38   [17]CICERO Center for International Climate Research, Oslo, Norway
39   [18]Statistics Division, Food and Agriculture Organization of the United Nations, Via Terme di
40   Caracalla, Rome, Italy
41   [19]Max Planck Institute for Biogeochemistry, Jena, Germany
42   [20]Sino-France Institute of Earth Systems Science, Laboratory for Earth Surface Processes,
43   College of Urban and Environmental Sciences, Peking University, Beijing, China
44   [21]Karlsruhe Institute of Technology, Institute of Meteorology and Climate Research/Atmospheric
45   Environmental Research, Garmisch-Partenkirchen, Germany

46 [22]Climate and Environmental Physics, Physics Institute and Oeschger Centre for Climate Change
47 Research, University of Bern, Bern, Switzerland
48 [23]Centre National de Recherches Météorologiques (CNRM), Université de Toulouse, Météo-
49 France, CNRS, Toulouse, France
50 [24]LMD-IPSL, Ecole Normale Supérieure / PSL Université, CNRS; Ecole Polytechnique,
51 Sorbonne Université, Paris, France
52 [25]PBL Netherlands Environmental Assessment Agency, The Hague, The Netherlands
53 [26]Department of Earth Sciences – Geochemistry, Faculty of Geosciences, Utrecht University,
54 Utrecht, The Netherlands
55 [27]Key Laboratory of Marine Chemistry Theory and Technology, Ministry of Education, Ocean
56 University of China, Qingdao, China
57 [28]Tyndall Centre for Climate Change Research, School of Environmental Sciences, University of
58 East Anglia, Norwich, UK
59 [29]College of Environmental and Resource Sciences, Zhejiang University, Hangzhou, China.
60 [30]National Centre for Earth Observation, University of Leeds, Leeds, UK
61 [31]Institute for Climate and Atmospheric Science, School of Earth and Environment, University of
62 Leeds, Leeds, UK
63 [32]Woods Hole Research Center, Falmouth, MA, USA
64 [33]NOAA Global Monitoring Laboratory, Boulder, CO, USA
65 [34]Centre for Coastal Biogeochemistry, School of Environment Science and Engineering,
66 Southern Cross University, Lismore, New South Wales, Australia
67 [35]Faculty of Geographical Science, Beijing Normal University, Beijing, China
68 [36]Center for Global Environmental Research, National Institute for Environmental Studies,
69 Tsukuba, Japan
70 [37]Climate Science Centre, CSIRO Oceans and Atmosphere, Aspendale, Victoria, Australia
71 [38] GEOMAR Helmholtz Centre for Ocean Research Kiel, Kiel, Germany
72 [39]Istituto di Scienze Marine, Consiglio Nazionale delle Ricerche (CNR), Rome, Italy
73 [40]Université Paris-Saclay, INRAE, AgroParisTech, UMR ECOSYS, Thiverval-Grignon, France
74 [41]Ministry of Education Key Laboratory for Earth System modeling, Department of Earth
75 System Science, Tsinghua University, Beijing, China
76 [42]Yale School of Forestry and Environmental Studies, New Haven, CT, USA
77 [43]Land Economy, Environment & Society, Scotland's Rural College (SRUC), Edinburgh, UK
78 [44]Department of Soil, Water, and Climate, University of Minnesota, St Paul, MN, USA
79 [45]Department of Physical Geography and Ecosystem Science, Lund University, Lund, Sweden
80 [46]Research Institute for Global Change, JAMSTEC, Yokohama, Japan
81 [47]Center for Environmental Remote Sensing, Chiba University, Chiba, Japan
82 [48]Center for Global Change Science, Massachusetts Institute of Technology, Cambridge, MA,
83 USA
84 [49]Faculty of Science, Vrije Universiteit, Amsterdam, Netherlands.
85 [50] Scripps Institution of Oceanography, University of California San Diego, La Jolla, USA
86 [51]Department of Forestry, Mississippi State University, Mississippi State, MS, USA
87
88
89
90

91   Nitrous oxide (N_2O), like carbon dioxide, is a long-lived greenhouse gas that accumulates in

92   the atmosphere. The increase in atmospheric N_2O concentrations over the past 150 years

93   has contributed to stratospheric ozone depletion[1] and climate change[2]. Current national

94   inventories do not provide a full picture of N_2O emissions owing to their omission of

95   natural sources and the limitations in methodology for attributing anthropogenic sources.

96   In order to understand the steadily increasing atmospheric burden (about 2 percent per

97   decade) and develop effective mitigation strategies, it is essential to improve quantification

98   and attribution of natural and anthropogenic contributions and their uncertainties. Here

99   we present a global N_2O inventory that incorporates both natural and anthropogenic

100   sources and accounts for the interaction between nitrogen additions and the biochemical

101   processes that control N_2O emissions. We use bottom-up (inventory; statistical

102   extrapolation of flux measurements; process-based land and ocean modelling) and top-

103   down (atmospheric inversion) approaches to provide a comprehensive quantification of

104   global N_2O sources and sinks resulting from 21 natural and human sectors between 1980

105   and 2016. Global N_2O emissions were 17.0 (minimum-maximum: 12.2–23.5) teragrams of

106   nitrogen per year (bottom-up) and 16.9 (15.9–17.7) teragrams of nitrogen per year (top-

107   down) between 2007 and 2016. Global human-induced emissions, which are dominated by

108   nitrogen additions to croplands, increased by 30% over the past four decades to 7.3 (4.2–

109   11.4) teragrams of nitrogen per year. This increase was mainly responsible for the growth

110   in the atmospheric burden. Our findings point to growing N_2O emissions in emerging

111   economies—particularly Brazil, China and India. Analysis of process-based model

112   estimates reveals an emerging N_2O–climate feedback resulting from interactions between

113   nitrogen additions and climate change. The recent growth in N_2O emissions exceeds some

114 **of the highest projected emission scenarios[3,4], underscoring the urgency to mitigate N₂O**

115 **emissions.**

116

117 Nitrous oxide (N₂O) is a long-lived stratospheric ozone-depleting substance and greenhouse gas

118 (GHG) with a current atmospheric lifetime of 116 ± 9 years (ref. [1]). The concentration of

119 atmospheric N₂O has increased by over 20% from 270 parts per billion (ppb) in 1750 to 331 ppb

120 in 2018 (Extended Data Fig. 1), with the fastest growth observed in the past five decades[5,6]. Two

121 key biochemical processes, nitrification and denitrification, control N₂O production in both

122 terrestrial and aquatic ecosystems, and are regulated by multiple environmental and biological

123 factors, such as temperature, water, oxygen, acidity, substrate availability[7], particularly nitrogen

124 (N) fertilizer use and livestock manure management, and recycling[8-10]. In the coming decades,

125 N₂O emissions are expected to continue increasing due to the growing demand for food, feed,

126 fiber and energy, and a rising source from waste generation and industrial processes[4,11,12]. Since

127 1990, anthropogenic N₂O emissions have been annually reported by Annex I Parties to the

128 United Nations Framework Convention on Climate Change (UNFCCC). More recently, over 190

129 national signatories to the Paris Agreement are now required to report biannually their national

130 GHG inventory with sufficient detail and transparency to track progress towards their Nationally

131 Determined Contributions. Yet, these inventories do not provide a full picture of N₂O emissions

132 due to their omission of natural sources, the limitations in methodology for attributing

133 anthropogenic sources, and missing data for a number of key regions (e.g., South America,

134 Africa)[2,9,13]. Moreover, we need a complete account of all human activities that accelerate the

135 global N cycle and that interact with the biochemical processes controlling the fluxes of N₂O in

136 both terrestrial and aquatic ecosystems[2,8]. Here we present a comprehensive, consistent analysis

137   and synthesis of the global N_2O budget across all sectors, including natural and anthropogenic

138   sources and sinks, using both bottom-up (BU) and top-down (TD) methods and their cross-

139   constraints. Our assessment enhances understanding of the global N cycle and will inform policy

140   development for N_2O mitigation, ideally helping to curb warming to levels consistent with the

141   long-term goal of the Paris Agreement.

142   A reconciling framework (described in Extended Data Fig. 2) was utilized to take full

143   advantage of BU and TD approaches in estimating and constraining sources and sinks of N_2O.

144   BU approaches include emission inventories, spatial extrapolation of field flux measurements,

145   nutrient budget modeling, and process-based modeling for land and ocean fluxes. The TD

146   approaches combine measurements of N_2O mole fractions with atmospheric transport models in

147   statistical optimization frameworks (inversions) to constrain the sources. Here we constructed a

148   total of 43 flux estimates including 30 with BU approaches, five with TD approaches, and eight

149   other estimates with observation and modeling approaches (see Methods; Extended Data Fig. 2).

150   With this extensive data and BU/TD framework, we establish the most comprehensive global

151   and regional N_2O budgets that include 18 sources and different versions of its chemical sink,

152   which are further grouped into six categories (Fig. 1 and Table 1): 1) Natural sources (no

153   anthropogenic effects) including a very small biogenic surface sink, 2) Perturbed fluxes from

154   ecosystems induced by changes in climate, carbon dioxide (CO_2) and land cover, 3) Direct

155   emissions of N additions in the agricultural sector (Agriculture), 4) Other direct anthropogenic

156   sources, which include fossil fuel and industry, waste and waste water, and biomass burning, 5)

157   Indirect emissions from ecosystems that are either downwind or downstream from the initial

158   release of reactive N into the environment, which include N_2O release following transport and

159   deposition of anthropogenic N via the atmosphere or water bodies as defined by the

160   Intergovernmental Panel on Climate Change (IPCC)[14], and 6) The atmospheric chemical sink

161   with one value derived from observations and the other (TD) from the inversion models. To

162   quantify and attribute the regional N_2O budget, we further partition the Earth's ice-free land into

163   ten regions (Fig. 2 and Supplementary Fig. 1). With the construction of these budgets, we

164   explore the relative temporal and spatial importance of multiple sources and sinks driving the

165   atmospheric burden of N_2O, their uncertainties, and interactions between anthropogenic forcing

166   and natural fluxes of N_2O as an emerging climate feedback.

167

168   **The Global N_2O Budget (2007−2016)**

169   The BU and TD approaches give consistent estimates of global total N_2O emissions in the recent

170   decade to well within their respective uncertainties, with values of 17.0 (min-max: 12.2−23.5) Tg

171   N yr^{-1} and 16.9 (15.9−17.7) Tg N yr^{-1} for BU and TD sources, respectively. The global calculated

172   atmospheric chemical sink (i.e., N_2O losses via photolysis and reaction with $O(^1D)$ in the

173   troposphere and stratosphere) is 13.5 (12.4−14.6) Tg N yr^{-1}. The imbalance of sources and sinks

174   of N_2O derived from the averaged BU and TD estimates is 4.1 Tg N yr^{-1}. This imbalance agrees

175   well with the observed 2007−2016 increase in atmospheric abundance of 3.8−4.8 Tg N yr^{-1} (see

176   Methods). Natural sources from soils and oceans contributed 57% of total emissions (mean: 9.7;

177   min-max: 8.0−12.0 Tg N yr^{-1}) for the recent decade according to our BU estimate. We further

178   estimate the natural soil flux at 5.6 (4.9−6.5) Tg N yr^{-1} and the ocean flux at 3.4 (2.5−4.3) Tg N

179   yr^{-1} (see Methods).

180   Anthropogenic sources contributed on average 43% to the total N_2O emission (mean: 7.3;

181   min-max: 4.2−11.4 Tg N yr^{-1}), in which direct and indirect emissions from N additions in

182   agriculture and other sectors contributed ~52% and ~18%, respectively. Of the remaining

183   anthropogenic emissions, ~27% were from other direct anthropogenic sources including fossil

184   fuel and industry (~13%), with ~3% from perturbed fluxes caused by climate/CO_2/land cover

185   change.

186

187   **Four Decades of the Global N_2O Budget**

188   The atmospheric N_2O burden increased from 1462 Tg N in the 1980s to 1555 Tg N in the recent

189   decade, with a possible uncertainty ±20 Tg N. Our results (Table 1) demonstrate that global N_2O

190   emissions have also significantly increased, primarily driven by anthropogenic sources, with

191   natural sources relatively steady throughout the study period. Our BU and TD global N_2O

192   emissions are comparable in magnitude during 1998–2016, but TD results imply a larger inter-

193   annual variability (1.0 Tg N yr^{-1}; Extended Data Fig. 3a). BU and TD approaches diverge in the

194   magnitude of land versus ocean emissions, although they are consistent with respect to trends.

195   Specifically, the BU land estimate during 1998–2016 was on average 1.8 Tg N yr^{-1} higher than

196   the TD estimate, but showed a slightly slower increasing rate of 0.8±0.2 Tg N yr^{-1} per decade

197   (95% confidence interval; $P < 0.05$) compared to 1.1±0.6 Tg N yr^{-1} per decade ($P < 0.05$) from

198   TD (Extended Data Fig. 3b). Since 2005, the difference in the magnitude of emissions between

199   the two approaches has become smaller due to a large TD-inferred emission increase,

200   particularly in South America, Africa, and East Asia (Extended Data Fig. 3d, f, i). Oceanic N_2O

201   emissions from BU [3.6 (2.7–4.5) Tg N yr^{-1}] indicate a slight decline at a rate of 0.06 Tg N yr^{-1}

202   per decade ($P < 0.05$), while the TD approach gave a higher but stable value of 5.1 (3.4−7.1) Tg

203   N yr^{-1} during 1998–2016 (Table 1).

204   Based on BU approaches, anthropogenic N_2O emissions increased from 5.6 (3.6−8.7) Tg N yr^{-}

205   ^{1} in the 1980s to 7.3 (4.2−11.4) Tg N yr^{-1} in the recent decade at a rate of 0.6±0.2 Tg N yr^{-1} per

206   decade ($P < 0.05$). Up to 87% of this increase is from direct emission from agriculture (71%) and

207   indirect emission from anthropogenic N additions into soils (16%). Direct soil emission from

208   fertilizer applications is the major source for agricultural emission increases, followed by a small

209   but significant increase in emissions from livestock manure and aquaculture. The model-based

210   estimates of direct soil emissions[15-17] exhibit a faster increase than the three inventories used in

211   our study (see Methods; Extended Data Fig. 4a), which is largely attributed to the interactive

212   effects between climate change and N additions as well as spatio-temporal variability in

213   environmental factors such as rainfall and temperature that modulate the N_2O yield from

214   nitrification and denitrification. This result is in line with the elevated emission factor (EF)

215   deduced from the TD estimates, in which the inversion-based soil emissions increased at a faster

216   rate than suggested by the IPCC Tier 1 EF[14] (which assumes a linear response), especially after

217   2009 (ref. [18]). The remaining causes of the increase are attributed to other direct anthropogenic

218   sources (6%) and perturbed fluxes from climate/CO_2/land cover change (8%). The part of fossil

219   fuel and industry emissions decreased rapidly over 1980–2000 largely due to the installation of

220   emissions abatement equipment in industrial facilities producing nitric and adipic acid. However,

221   after 2000 such emissions began to increase slowly due to rising fossil fuel combustion

222   (Extended Data Fig. 5a-b).

223   Our analysis of process-based model estimates indicates that soil N_2O emissions accelerated

224   substantially due to climate change since the early 1980s, which has offset the reduction due to

225   elevated CO_2 concentration (Extended Data Fig. 6a). Elevated CO_2 enhances plant growth and

226   thus increases N uptake, which in turn decreases soil N_2O emissions[16,19]. Land conversion from

227   tropical mature forests with higher N_2O emissions to pastures and other unfertilized agricultural

228   lands has significantly reduced global natural N_2O emissions[11,20,21]. This decrease, however, was

229   partly offset by an increase in soil N_2O emissions attributable to the temporary rise of emissions

230   following deforestation (post-deforestation pulse effect) and background emissions from

231   converted croplands or pastures[21] (see Methods; Extended Data Fig. 7).

232   From the ensemble of process-based land model emissions[15,16], we estimate a global

233   agricultural soil EF of 1.8% (1.3%−2.3%), which is significantly larger than the IPCC Tier-1

234   default for direct emission of 1%. This higher EF, derived from process-based models, suggests a

235   strong interactive effect between N additions and other global environmental changes (Table 1,

236   Perturbed fluxes from climate, atmospheric CO_2, and land cover change). Previous field

237   experiments reported a better fit to local observations of soil N_2O emissions when assuming a

238   non-linear response to fertilizer N inputs under varied climate and soil conditions[17,22]. The non-

239   linear response is likely also associated with long-term N accumulation in agricultural soils from

240   N fertilizer use and in aquatic systems from N loads (the legacy effect)[18,23], which provides more

241   substrate for microbial processes[18,24]. The increasing N_2O emissions estimated by process-based

242   models[16] also suggest that recent climate change (particularly warming) may have boosted soil

243   nitrification and denitrification processes, contributing to the growing trend in N_2O emissions

244   together with rising N additions to agricultural soils[16,25-27] (Extended Data Fig. 8).

245

246   **Regional N_2O Budgets (2007−2016)**

247   BU approaches give estimates of N_2O emissions in the five source categories, while TD

248   approaches only provide total emissions (Fig. 2). BU and TD approaches indicate that Africa was

249   the largest N_2O source in the last decade, followed by South America (Fig. 2). BU and TD

250   approaches agree well in the magnitudes and trends of N_2O emissions from South Asia and

251   Oceania (Extended Data Fig. 3j, l). For the remaining regions, BU and TD estimates are

252   comparable in their trends but diverge in their source strengths. Clearly, much more work on

253   regional N_2O budgets is needed, particularly for South America and Africa where we see larger

254   differences between BU and TD estimates and larger uncertainty in each approach. Advancing

255   the understanding and model representation of key processes responsible for N_2O emissions from

256   land and ocean are priorities for reducing uncertainties in BU estimates. Atmospheric

257   observations in underrepresented regions of the world and better atmospheric transport models

258   are essential for uncertainty reduction in TD estimates, while more accurate activity data and

259   robust EFs are critical for GHG inventories (See Methods for additional discussion on

260   uncertainty).

261   Based on the Global N_2O Model Intercomparison Project (NMIP) estimates[16], natural soil

262   emissions (to different extents) dominated in tropical and sub-tropical regions. Soil N_2O

263   emissions in the tropics (0.1 ± 0.04 g N m^{-2} yr^{-1}) are about 50% higher than the global average,

264   since many lowland, highly-weathered tropical soils have excess N relative to phosphorus[20].

265   Total anthropogenic emissions in the ten terrestrial regions were highest in East Asia (1.5;

266    $0.8-2.6$ Tg N yr^{-1}), followed by North America, Africa, and Europe. High direct agricultural N_2O

267   emissions can be attributed to large-scale synthetic N fertilizer applications in East Asia, Europe,

268   South Asia, and North America, which together consume over 80% of the world's synthetic N

269   fertilizers[28]. In contrast, direct agricultural emissions from Africa and South America are mainly

270   induced by livestock manure that is deposited in pastures and rangelands[28,29]. East Asia

271   contributed 71%−79% of global aquaculture N_2O emissions; South Asia and Southeast Asia

272   together contributed 10%−20% (refs. [30,31]). Indirect emissions play a moderate role in the total

273   N_2O budget, with the highest emission in East Asia (0.3; 0.1−0.5 Tg N yr^{-1}). Other direct

274   anthropogenic sources together contribute N_2O emissions of approximately 0.2−0.4 Tg N yr^{-1} in

275   East Asia, Africa, North America, and Europe.

276   Both BU and TD estimates of ocean N_2O emissions for northern, tropical, and southern ocean

277   regions (90°−30°N, 30°N−30°S, and 30°−90°S, respectively) reveal that the tropical oceans

278   contribute over 50% to the global oceanic source. In particular, the upwelling regions of the

279   equatorial Pacific, Indian and tropical Atlantic (Fig. 3) provide significant sources of N_2O[32-34].

280   BU estimates suggest the southern ocean is the second largest regional contributor with

281   emissions about twice as high as from the northern oceans (53% tropical oceans, 31% southern

282   oceans, 17% northern oceans), in line with their area, while the TD estimates suggest

283   approximately equal contributions from the southern and northern oceans.

284

285   **Four Decades of Anthropogenic N_2O Emissions**

286   Trends in anthropogenic emissions varied among regions (Fig. 3). Fluxes from Europe and

287   Russia decreased by a total of 0.6 (0.5−0.7) Tg N yr^{-1} over the past 37 years (1980−2016). The

288   decrease in Europe is associated with successful emissions abatement in industry as well as

289   agricultural policies, while the decrease in Russia is associated with the collapse of the

290   agricultural cooperative system after 1990. In contrast, fluxes from the remaining eight regions

291   increased by a total of 2.9 (2.4−3.4) Tg N yr^{-1} (Fig. 3), of which 34% came from East Asia, 18%

292   from Africa, 18% from South Asia, 13% from South America, only 6% from North America,

293   and with remaining increases due to other regions.

294   The relative importance of each anthropogenic source to the total emission increase differs

295   among regions. East Asia, South Asia, Africa, and South America show larger increases in total

296   agricultural N_2O emissions (direct and indirect) compared to the remaining six regions during

297   1980−2016 (Fig. 3). Southeast Asia, North America, and Middle East also show increasing direct

298   N_2O emissions but to smaller extent. Rising indirect emissions in these four regions (East Asia,

299   South Asia, Africa, and South America) on average constitute 20% of total agricultural N_2O

300   emissions and are largely induced by the considerable increase in fertilizer N inputs to

301   agricultural soils[35,36]. The most rapid increase in emissions from other direct anthropogenic

302   sources was found in East Asia, primarily owing to the fast-growing industrial emissions. Africa

303   and South Asia show a fast emission increase due to emissions from fossil fuel and industry and

304   waste and waste water.

305   Our findings point to growing N_2O emissions in emerging economies, particularly Brazil,

306   China, and India. For example, we find here that the substantial increases in livestock manure

307   left on pasture and in fertilizer use caused a ~120% increase in Brazilian agricultural N_2O

308   emissions during 1980−2016 (Extended Data Fig. 9). In addition to fertilizer applications, global

309   livestock manure production has been growing steadily, in line with increased livestock

310   numbers[15,28]. Rising demand for meat and dairy products has significantly increased global N_2O

311   emissions from livestock manure production and management associated with the expansion of

312   pastures and grazing land[37]. Meanwhile, expansion of feed crop production to support the growth

313   of livestock could further enhance global N_2O emissions[37,38]. Likewise, increasing demand for

314   fish has triggered a five-fold increase in global aquaculture production since the late 1980s[39],

315   with demand projected to increase further[40], although this remains a small fraction (<1%) of total

316   N_2O emissions.

317   The acceleration of global N_2O emissions resulting from anthropogenic sources is apparent in

318   both BU and TD results and currently tracks the highest Representative Concentration Pathway

319   (RCP8.5)[4] in the fifth assessment report (AR5) of IPCC[2] and exceeds all the Shared

12

320   Socioeconomic Pathways (SSPs)[3] in CMIP6 for the sixth assessment report (AR6) of IPCC (Fig.

321   4). Observed atmospheric N_2O concentrations are beginning to exceed predicted levels across all

322   scenarios. Emissions need to be reduced to a level that is consistent with or below that in RCP2.6

323   or SSP1-2.6 in order to limit warming well below the 2°C target of the Paris Agreement. Failure

324   to include N_2O within climate mitigation strategies will necessitate even greater abatement of

325   CO_2 and CH_4. Although N_2O mitigation is difficult because N is the key-limiting nutrient in the

326   agricultural production, this study demonstrates that effective mitigation actions have reduced

327   emissions in some regions, such as Europe, through technological improvements in industry and

328   improved N use efficiency in agriculture.

329   There are a number of mitigation options in the agriculture sector available for immediate

330   deployment, including increased N use efficiency in (i) animal production through tuning of feed

331   rations to reduce N excretion, and (ii) in crop production through precision delivery of N

332   fertilizers, split applications and better timing to match N applications to crop demand,

333   conservation tillage, prevention of waterlogging, and the use of nitrification inhibitors[43,44].

334   Success stories include the stabilization or reduction of N_2O emissions through improving N use

335   efficiency in the United States and Europe, while maintaining or even increasing crop yields[44,45].

336   There is every reason to expect that additional implementation of more sustainable practices and

337   emerging technologies will lead to further reductions in these regions. For example, N_2O

338   emissions from European agricultural soils decreased by 21% between 1990 and 2010, a decline

339   attributable to the implementation of the Nitrates Directive (an agricultural policy favoring

340   optimization and reduction of fertilizer use as well as water protection legislation)[46]. For regions

341   where emissions are growing, an immediate opportunity lies in the reduction of excess fertilizer

342   use along with the implementation of more sustainable agricultural practices that together have

343   been shown to increase crop yields, reduce N_2O emissions, increase water quality, and increase

344   farm income[47]. In addition, N_2O emissions can be efficiently abated in the chemical

345   industry[11,43,48,49], as has been achieved successfully in nitric acid plants in the European Union

346   where industrial N_2O emissions dropped from 11% to 3% of total emissions between 2007 and

347   2012 (ref. [46]). Additional available strategies to reduce N_2O emissions include promoting lower

348   meat consumption in some parts of the world[9] and reducing food waste[11].

349   We present the most comprehensive global N_2O budget to date, with a detailed sectorial and

350   regional attribution of sources and sinks. Each of the past four decades had higher global N_2O

351   emissions than the previous one, and in all, agricultural activities dominated the growth in

352   emissions. Total industrial emissions have been quite stable with increased emissions from the

353   fossil fuel sector offset to some extent by the decline in emissions in other industrial sectors as a

354   result of successful abatement policies. We also highlight a number of complex interactions

355   between N_2O fluxes and human-driven changes whose impact on the global atmospheric N_2O

356   growth rate was previously unknown. Those interactions include the effects of climate change,

357   increasing atmospheric CO_2, and deforestation. Cumulatively, these exert a relatively small

358   effect on the overall N_2O growth, however, individual flux components, such as the growing

359   positive climate-N_2O feedback, are significant. These fluxes are not currently included in the

360   national GHG reporting. We further find that Brazil, China, and India dominate the regional

361   contributions to the increase in global N_2O emissions over the most recent decade. Our extensive

362   database and modelling capability fill current gaps in national and regional emissions

363   inventories. Future research is needed to further constrain complex biogeochemical interactions

364   between natural/anthropogenic fluxes and global environmental changes, which could lead to

365   significant feedbacks in the future. Reducing excess N applications to croplands and adopting

366 precision fertilizer application methods provide the largest immediate opportunities for N$_2$O

367 emissions abatement.

368

369 **References**

370 1   Prather, M. J. *et al.* Measuring and modeling the lifetime of nitrous oxide including its
371   variability. *Journal of Geophysical Research: Atmospheres* **120**, 5693-5705 (2015).
372 2   Ciais, P. *et al.* in *Climate Change 2013: The Physical Science Basis. Contribution of*
373   *Working Group I to the Fifth Assessment Report of the Intergovernmental Panel on*
374   *Climate Change* 465-570 (Cambridge University Press, 2014).
375 3   Gidden, M. J. *et al.* Global emissions pathways under different socioeconomic scenarios
376   for use in CMIP6: a dataset of harmonized emissions trajectories through the end of the
377   century. *Geoscientific Model Development* **12**, 1443-1475 (2019).
378 4   Davidson, E. A. Representative concentration pathways and mitigation scenarios for
379   nitrous oxide. *Environmental Research Letters* **7**, 024005 (2012).
380 5   Hall, B., Dutton, G. & Elkins, J. The NOAA nitrous oxide standard scale for atmospheric
381   observations. *Journal of Geophysical Research: Atmospheres* **112**, D09305 (2007).
382 6   Prinn, R. G. *et al.* History of chemically and radiatively important atmospheric gases
383   from the Advanced Global Atmospheric Gases Experiment (AGAGE). *Earth System*
384   *Science Data* **10**, 985-1018 (2018).
385 7   Butterbach-Bahl, K., Baggs, E. M., Dannenmann, M., Kiese, R. & Zechmeister-
386   Boltenstern, S. Nitrous oxide emissions from soils: how well do we understand the
387   processes and their controls? *Phil. Trans. R. Soc. B* **368**, 20130122 (2013).
388 8   Tian, H. *et al.* The terrestrial biosphere as a net source of greenhouse gases to the
389   atmosphere. *Nature* **531**, 225-228 (2016).
390 9   UNEP. Drawing down N$_2$O to protect climate and the ozone layer. Report No.
391   9280733583, (United Nations Environment Programme (UNEP), 2013).
392 10   Park, S. *et al.* Trends and seasonal cycles in the isotopic composition of nitrous oxide
393   since 1940. *Nature Geoscience* **5**, 261-265 (2012).
394 11   Davidson, E. A. & Kanter, D. Inventories and scenarios of nitrous oxide emissions.
395   *Environmental Research Letters* **9**, 105012 (2014).
396 12   Reay, D. S. *et al.* Global agriculture and nitrous oxide emissions. *Nature Climate Change*
397   **2**, 410-416 (2012).
398 13   Syakila, A. & Kroeze, C. The global nitrous oxide budget revisited. *Greenhouse Gas*
399   *Measurement and Management* **1**, 17-26 (2011).
400 14   IPCC. 2006 IPCC Guidelines for National Greenhouse Gas Inventories., (Japan on behalf
401   of the IPCC, Hayama, Japan, 2006).
402 15   Dangal, S. R. *et al.* Global nitrous oxide emissions from pasturelands and rangelands:
403   Magnitude, spatio-temporal patterns and attribution. *Global Biogeochemical Cycles* **33**,
404   200-222 (2019).
405 16   Tian, H. Q. *et al.* Global soil nitrous oxide emissions since the preindustrial era estimated
406   by an ensemble of terrestrial biosphere models: Magnitude, attribution, and uncertainty.
407   *Global Change Biology* **25**, 640-659 (2019).

408 17 Wang, Q. *et al.* Data-driven estimates of global nitrous oxide emissions from croplands.
409 *National Science Review* **7**, 441-452 (2020).
410 18 Thompson, R. L. *et al.* Acceleration of global N_2O emissions seen from two decades of
411 atmospheric inversion. *Natural Climate Change* **9**, 993-998 (2019).
412 19 Zaehle, S., Ciais, P., Friend, A. D. & Prieur, V. Carbon benefits of anthropogenic reactive
413 nitrogen offset by nitrous oxide emissions. *Nature Geoscience* **4**, 601-605 (2011).
414 20 Davidson, E. A. *et al.* Recuperation of nitrogen cycling in Amazonian forests following
415 agricultural abandonment. *Nature* **447**, 995-998 (2007).
416 21 Verchot, L. V. *et al.* Land use change and biogeochemical controls of nitrogen oxide
417 emissions from soils in eastern Amazonia. *Global Biogeochemical Cycles* **13**, 31-46
418 (1999).
419 22 Shcherbak, I., Millar, N. & Robertson, G. P. Global metaanalysis of the nonlinear
420 response of soil nitrous oxide (N_2O) emissions to fertilizer nitrogen. *Proceedings of the*
421 *National Academy of Sciences* **111**, 9199-9204 (2014).
422 23 Van Meter, K. J., Basu, N. B., Veenstra, J. J. & Burras, C. L. The nitrogen legacy:
423 emerging evidence of nitrogen accumulation in anthropogenic landscapes. *Environmental*
424 *Research Letters* **11**, 035014 (2016).
425 24 Firestone, M. K. & Davidson, E. A. Microbiological basis of NO and N_2O production and
426 consumption in soil. *Exchange of trace gases between terrestrial ecosystems the*
427 *atmosphere* **47**, 7-21 (1989).
428 25 Griffis, T. J. *et al.* Nitrous oxide emissions are enhanced in a warmer and wetter world.
429 *Proceedings of the National Academy of Sciences* **114**, 12081-12085 (2017).
430 26 Pärn, J. *et al.* Nitrogen-rich organic soils under warm well-drained conditions are global
431 nitrous oxide emission hotspots. *Nature Communications* **9**, 1135 (2018).
432 27 Smith, K. The potential for feedback effects induced by global warming on emissions of
433 nitrous oxide by soils. *Global Change Biology* **3**, 327-338 (1997).
434 28 FAOSTAT. The Food and Agriculture Organization of the United Nations Statistics:
435 Emissions-Agriculture, Emissions Land Use Trade (Crops and livestock products),
436 Population, Agri-Environmental Indicators (Livestock Manure) (2019).
437 29 Xu, R. *et al.* Increased nitrogen enrichment and shifted patterns in the world's grassland:
438 1860–2016. *Earth System Science Data* **11**, 175-187 (2019).
439 30 Beusen, A. H., Bouwman, A. F., Van Beek, L. P., Mogollón, J. M. & Middelburg, J. J.
440 Global riverine N and P transport to ocean increased during the 20th century despite
441 increased retention along the aquatic continuum. *Biogeosciences* **13**, 2441-2451 (2016).
442 31 MacLeod, M., Hasan, M. R., Robb, D. H. F. & Mamun-Ur-Rashid, M. Quantifying and
443 mitigating greenhouse gas emissions from global aquaculture. *FAO, Rome* (2019).
444 32 Buitenhuis, E. T., Suntharalingam, P. & Le Quéré, C. Constraints on global oceanic
445 emissions of N_2O from observations and models. *Biogeosciences* **15**, 2161-2175 (2018).
446 33 Manizza, M., Keeling, R. F. & Nevison, C. D. On the processes controlling the seasonal
447 cycles of the air–sea fluxes of O_2 and N_2O: A modelling study. *Tellus B: Chemical and*
448 *Physical Meteorology* **64**, 18429 (2012).
449 34 Martinez-Rey, J., Bopp, L., Gehlen, M., Tagliabue, A. & Gruber, N. Projections of
450 oceanic N_2O emissions in the 21st century using the IPSL Earth system model.
451 *Biogeosciences* **12**, 4133-4148 (2015).
452 35 Maavara, T. *et al.* Nitrous oxide emissions from inland waters: Are IPCC estimates too
453 high? *Global Change Biology* **25**, 473-488 (2019).

454   36   Yao, Y. *et al.* Increased global nitrous oxide emissions from streams and rivers in the
455   Anthropocene. *Natural Climate Change* **10**, 138-142 (2020).

456   37   Gerber, P. J. *et al. Tackling climate change through livestock: a global assessment of*
457   *emissions and mitigation opportunities. FAO* (2013).

458   38   Herrero, M. *et al.* Biomass use, production, feed efficiencies, and greenhouse gas
459   emissions from global livestock systems. *Proceedings of the National Academy of*
460   *Sciences* **110**, 20888-20893 (2013).

461   39   Yuan, J. *et al.* Rapid growth in greenhouse gas emissions from the adoption of industrial-
462   scale aquaculture. *Nature Climate Change* **9**, 318-322 (2019).

463   40   Froehlich, H. E., Runge, C. A., Gentry, R. R., Gaines, S. D. & Halpern, B. S.
464   Comparative terrestrial feed and land use of an aquaculture-dominant world. *Proceedings*
465   *of the National Academy of Sciences* **115**, 5295-5300 (2018).

466   41   O'Neill, B. C. *et al.* The Scenario Model Intercomparison Project (ScenarioMIP) for
467   CMIP6. *Geoscience Model Development* **9**, 3461-3482 (2016).

468   42   Gütschow, J. *et al.* The PRIMAP-hist national historical emissions time series. *Earth*
469   *System Science Data* **8**, 571-603 (2016).

470   43   Winiwarter, W., Höglund-Isaksson, L., Klimont, Z., Schöpp, W. & Amann, M. Technical
471   opportunities to reduce global anthropogenic emissions of nitrous oxide. *Environmental*
472   *Research Letters* **13**, 014011 (2018).

473   44   Zhang, X. *et al.* Managing nitrogen for sustainable development. *Nature* **528**, 51-59
474   (2015).

475   45   Mueller, N. D. *et al.* Declining spatial efficiency of global cropland nitrogen allocation.
476   *Global Biogeochemical Cycles* **31**, 245-257 (2017).

477   46   European Environment Agency. Annual European Union greenhouse gas inventory 1990-
478   2017 and inventory report 2019. *Submission under the United Nations Framework*
479   *Convention on Climate Change and the Kyoto Protocol, Copenhagen, DK* (2019).

480   47   Cui, Z. *et al.* Pursuing sustainable productivity with millions of smallholder farmers.
481   *Nature* **555**, 363-366 (2018).

482   48   Kanter, D. *et al.* A post-Kyoto partner: considering the stratospheric ozone regime as a
483   tool to manage nitrous oxide. *Proceedings of the National Academy of Sciences* **110**,
484   4451-4457 (2013).

485   49   Schneider, L., Lazarus, M. & Kollmuss, A. J. S. M. S. E. I. Industrial N_2O projects under
486   the CDM: Adipic acid-A case of carbon leakage. *Stockholm Environment Institute*
487   (2010).

488

489

490

491

492

493

494

495

496 **Table 1 The global N₂O budget in the 1980s, 1990s, 2000s, and 2007–2016.**

		the 1980s			the 1990s			the 2000s			2007-2016		
Anthropogenic sources		mean	min	max	mean	min	max	mean	min	max	mean	min	max
Direct emissions of N additions in the agricultural sector (Agriculture)	Direct soil emissions	1.5	0.9	2.6	1.7	1.1	3.1	2.0	1.3	3.4	2.3	1.4	3.8
	Manure left on pasture	0.9	0.7	1.0	1.0	0.7	1.1	1.1	0.8	1.2	1.2	0.9	1.3
	Manure management	0.3	0.2	0.4	0.3	0.2	0.4	0.3	0.2	0.5	0.3	0.2	0.5
	Aquaculture	0.01	0.00	0.03	0.03	0.01	0.1	0.1	0.02	0.2	0.1	0.02	0.2
	sub-total	2.6	1.8	4.1	3.0	2.1	4.8	3.4	2.3	5.2	3.8	2.5	5.8
Other direct anthropogenic sources	Fossil fuel and industry	0.9	0.8	1.1	0.9	0.9	1.0	0.9	0.8	1.0	1.0	0.8	1.1
	Waste and waste water	0.2	0.1	0.3	0.3	0.2	0.4	0.3	0.2	0.4	0.3	0.2	0.5
	Biomass burning	0.7	0.7	0.7	0.7	0.6	0.8	0.6	0.6	0.6	0.6	0.5	0.8
	sub-total	1.8	1.6	2.1	1.9	1.7	2.1	1.8	1.6	2.1	1.9	1.6	2.3
Indirect emissions from anthropogenic N additions	Inland waters, estuaries, coastal zones	0.4	0.2	0.5	0.4	0.2	0.5	0.4	0.2	0.6	0.5	0.2	0.7
	Atmospheric N deposition on land	0.6	0.3	1.2	0.7	0.4	1.4	0.7	0.4	1.3	0.8	0.4	1.4
	Atmospheric N deposition on ocean	0.1	0.1	0.2	0.1	0.1	0.2	0.1	0.1	0.2	0.1	0.1	0.2
	sub-total	1.1	0.6	1.9	1.2	0.7	2.1	1.2	0.6	2.1	1.3	0.7	2.2
Perturbed fluxes from climate/CO₂/land cover change	CO₂ effect	-0.2	-0.3	0.0	-0.2	-0.4	0.0	-0.3	-0.5	0.1	-0.3	-0.6	0.1
	Climate effect	0.4	0.0	0.8	0.5	0.1	0.9	0.7	0.3	1.2	0.8	0.3	1.3
	Post-deforestation pulse effect	0.7	0.6	0.8	0.7	0.6	0.8	0.7	0.7	0.8	0.8	0.7	0.8
	Long-term effect of reduced mature forest area	-0.8	-0.8	-0.9	-0.9	-0.8	-1.0	-1.0	-0.9	-1.1	-1.1	-1.0	-1.1
	sub-total	0.1	-0.4	0.7	0.1	-0.5	0.7	0.2	-0.4	0.9	0.2	-0.6	1.1
Anthropogenic total		5.6	3.6	8.7	6.2	3.9	9.7	6.7	4.1	10.3	7.3	4.2	11.4
Natural fluxes													
Natural soils baseline		5.6	4.9	6.6	5.6	4.9	6.5	5.6	5.0	6.5	5.6	4.9	6.5
Ocean baseline		3.6	3.0	4.4	3.5	2.8	4.4	3.5	2.7	4.3	3.4	2.5	4.3
Natural (Inland waters, estuaries, coastal zones)		0.3	0.3	0.4	0.3	0.3	0.4	0.3	0.3	0.4	0.3	0.3	0.4
Lightning and atmospheric production		0.4	0.2	1.2	0.4	0.2	1.2	0.4	0.2	1.2	0.4	0.2	1.2
Surface sink		-0.01	0.00	-0.3	-0.01	0.00	-0.3	-0.01	0.00	-0.3	-0.01	0.00	-0.3
Natural total		9.9	8.5	12.2	9.8	8.3	12.1	9.8	8.2	12.0	9.7	8.0	12.0
Bottom-up total source		15.5	12.1	20.9	15.9	12.2	21.7	16.4	12.3	22.4	17.0	12.2	23.5
Top-down Ocean								5.1	3.1	7.2	5.1	3.4	7.1
Top-down Land								10.8	9.3	12.5	11.8	10.6	13.8
Top-down total source								15.9	15.1	16.9	16.9	15.9	17.7
Top-down Statospheric sink								12.1	11.4	13.1	12.4	11.7	13.3
Observed atmospheric chemical sink*								13.3	12.2	14.4	13.5	12.4	14.6
Change in atmospheric abundance**								**3.7**	**3.2**	**4.2**	**4.3**	**3.8**	**4.8**
Atmospheric burden		1462	1442	1482	1493	1472	1514	1531	1510	1552	1555	1533	1577

497 Note: *BU estimates include four categories of anthropogenic sources (red for agriculture, orange for*
498 *other direct anthropogenic sources, maroon for indirect emissions from anthropogenic N additions, and*
499 *brown for perturbed fluxes from climate/CO₂/land cover change) and one category for natural sources*
500 *and sinks (green). The sources and sinks of N₂O are given in Tg N yr⁻¹. The atmospheric burden is given*
501 *in Tg N. *calculated from satellite observations with a photolysis model (about 1% of this sink*
502 *occurs in the troposphere). **Calculated from the combined NOAA and AGAGE record of surface N₂O,*
503 *and adopting the uncertainty of the IPCC AR5 (Chapter 6)[2]. Detailed information on calculating each*
504 *sub-category is shown in Supplementary Tables 1–13.*

GLOBAL N₂O BUDGET
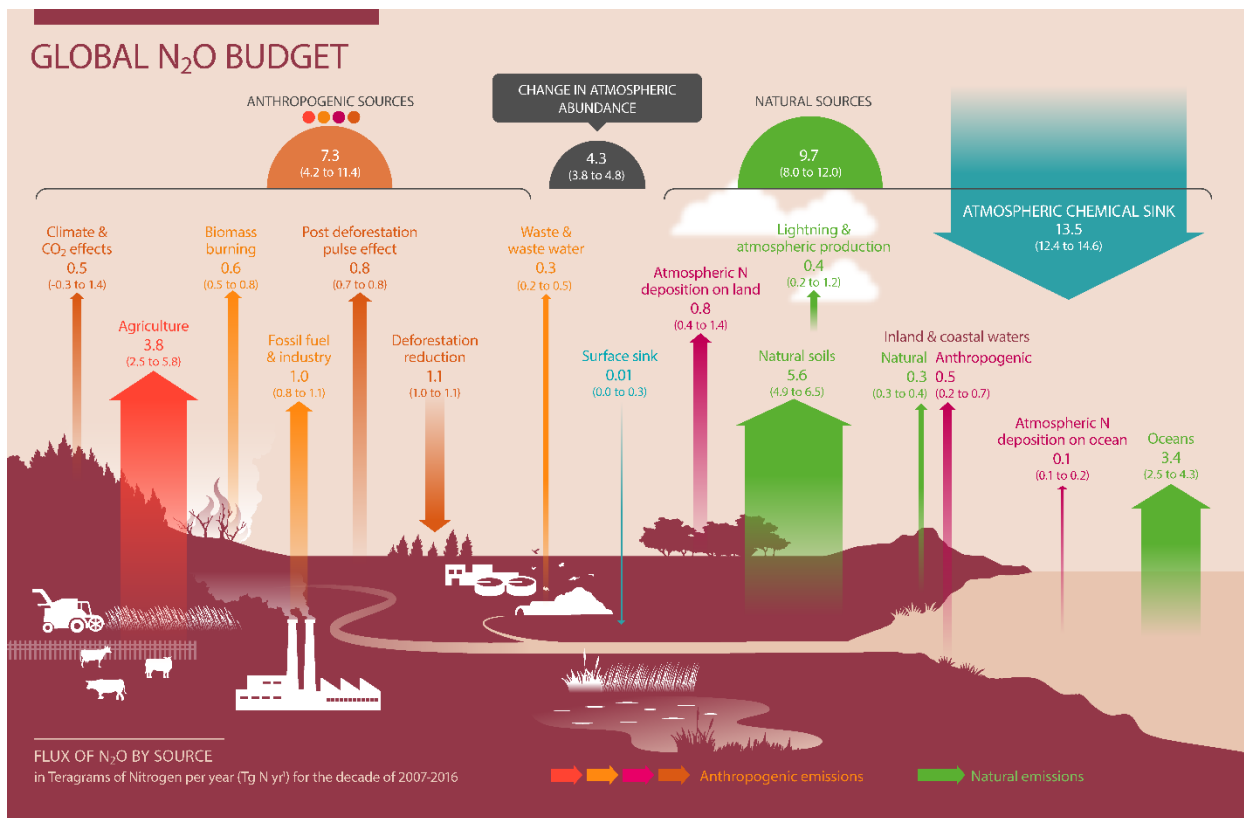
FLUX OF N₂O BY SOURCE
in Teragrams of Nitrogen per year (Tg N yr⁻¹) for the decade of 2007-2016

Fig. 1 Global N₂O budget for the recent decade (2007−2016). *The red arrow represents direct emissions of N additions in the agricultural sector (Agriculture). The orange arrows represent emissions from other direct anthropogenic sources. The maroon arrows represent indirect emissions from anthropogenic N additions. The brown arrows represent perturbed fluxes from climate/CO₂/land cover change effects. The green arrows represent natural source. The anthropogenic and natural N₂O sources are derived from BU estimates. The blue arrows represent surface sink and observed atmospheric chemical sink of which about 1% occurs in the troposphere. The total budget (sources + sinks) does not exactly match the observed atmospheric accumulation, because each of the terms has been derived independently and we do not force top-down agreement by rescaling the terms. This imbalance readily falls within the overall uncertainty in closing the N₂O budget, as reflected in each of the terms. The N₂O sources and sinks are given in Tg N yr⁻¹.*
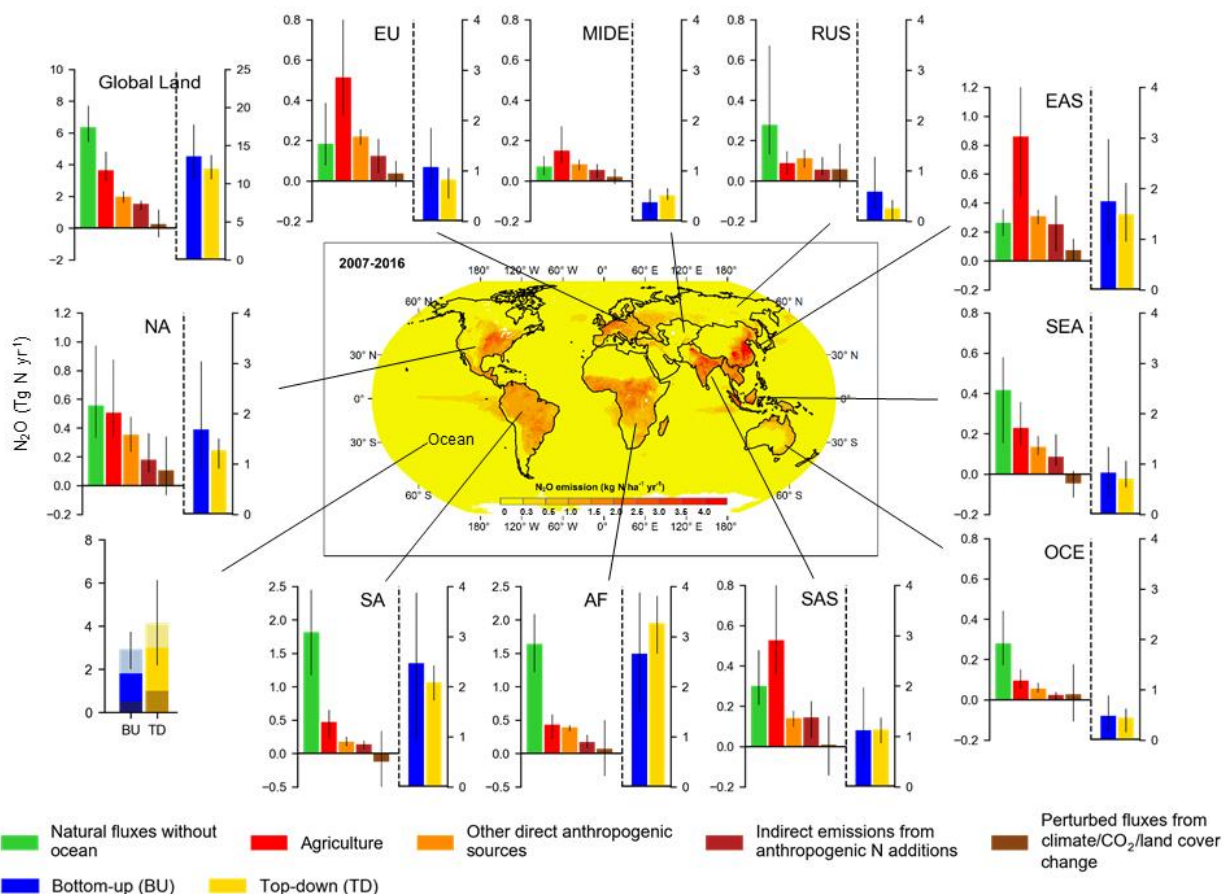
Fig. 2 Regional N$_2$O sources in the recent decade (2007−2016) over 11 regions. *The Earth's ice-free land is partitioned into ten regions: North America (NA), South America (SA), Europe (EU), Middle East (MIDE), Africa (AF), Russia (RUS), East Asia (EAS), South Asia (SAS), Southeast Asia (SEA), and Oceania (OCE). In each subplot from left to right: emissions from five sub-sectors using BU approaches: natural fluxes without ocean (green), direct emissions of N additions in the agricultural sector (Agriculture, red), other direct anthropogenic sources (orange), indirect emissions from anthropogenic N additions (maroon), and perturbed fluxes from climate/CO$_2$/land cover change (brown); the sum of these five categories by BU approaches (blue), and the estimates by TD approaches (gold). BU and TD estimates of ocean emissions are shown at the bottom left (from bottom to top: 30°−90°N, 30°S−30°N, and 90°−30°S). Error bars indicate the spread between the minimum and the maximum values. The center map shows the spatial distribution of 10-year average N$_2$O emissions from land and ocean based on the land and ocean models. Per capita N$_2$O emission (kg N capita^{-1} yr^{-1}) during 2007−2016 is shown in Supplementary Fig. 2.*

20
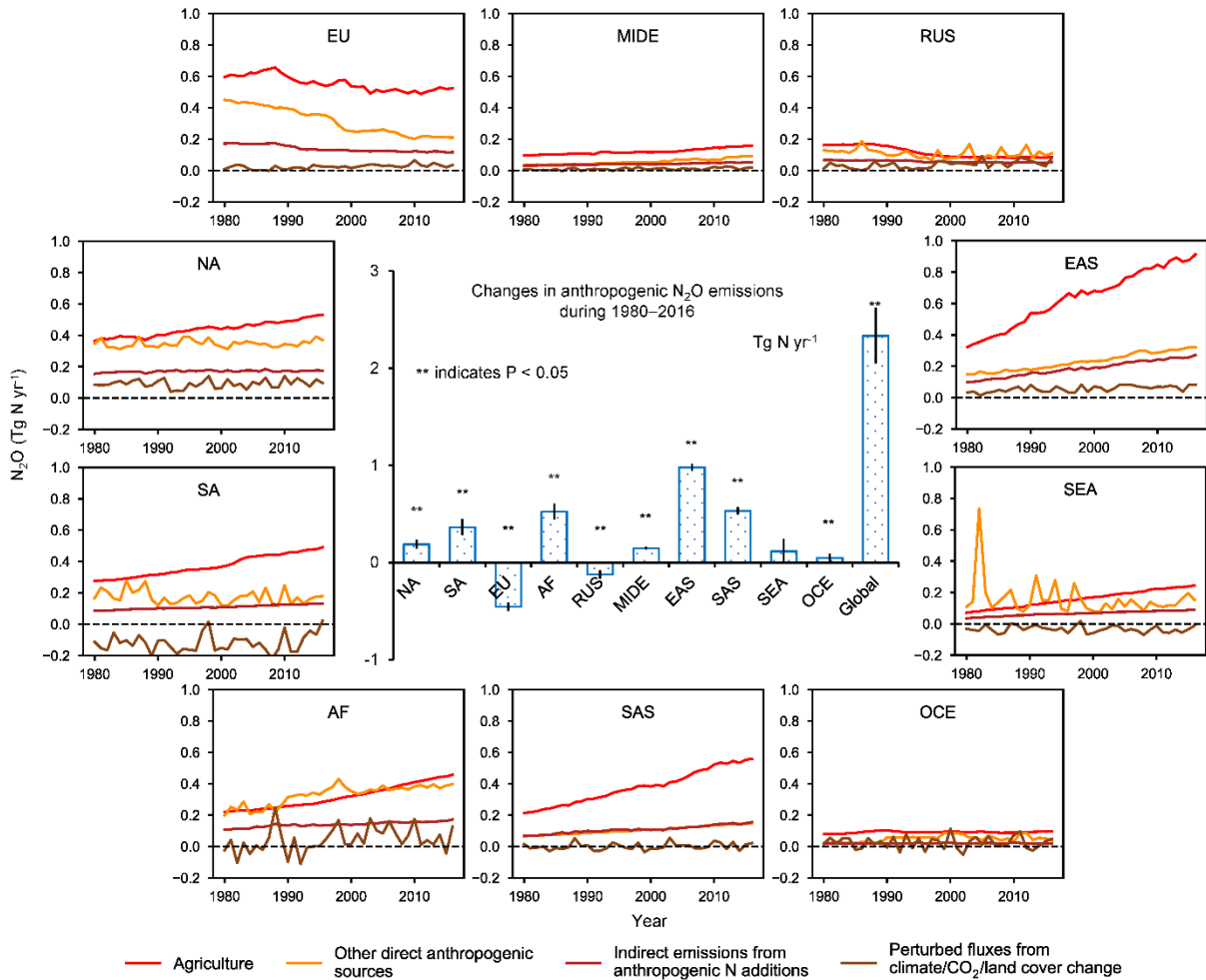
Fig. 3 Ensembles of regional anthropogenic N₂O emissions over the 1980–2016 period. *The bar chart in the center shows the accumulated changes in regional and global N₂O emissions during the study period. Error bars indicate the 95% confidence interval for the average of accumulated changes. The Mann-Kendall test was performed to examine a monotonic increasing or decreasing trend in the estimated ensemble N₂O emissions for each region and the globe during 1980–2016. The accumulated changes were calculated from the linear regressed annual change rate (Tg N yr⁻²) multiplied by 37 years. All regions except SEA show a significant increasing or decreasing trend in the estimated ensemble N₂O emissions during the study period (indicated by ∗∗ for each bar).*
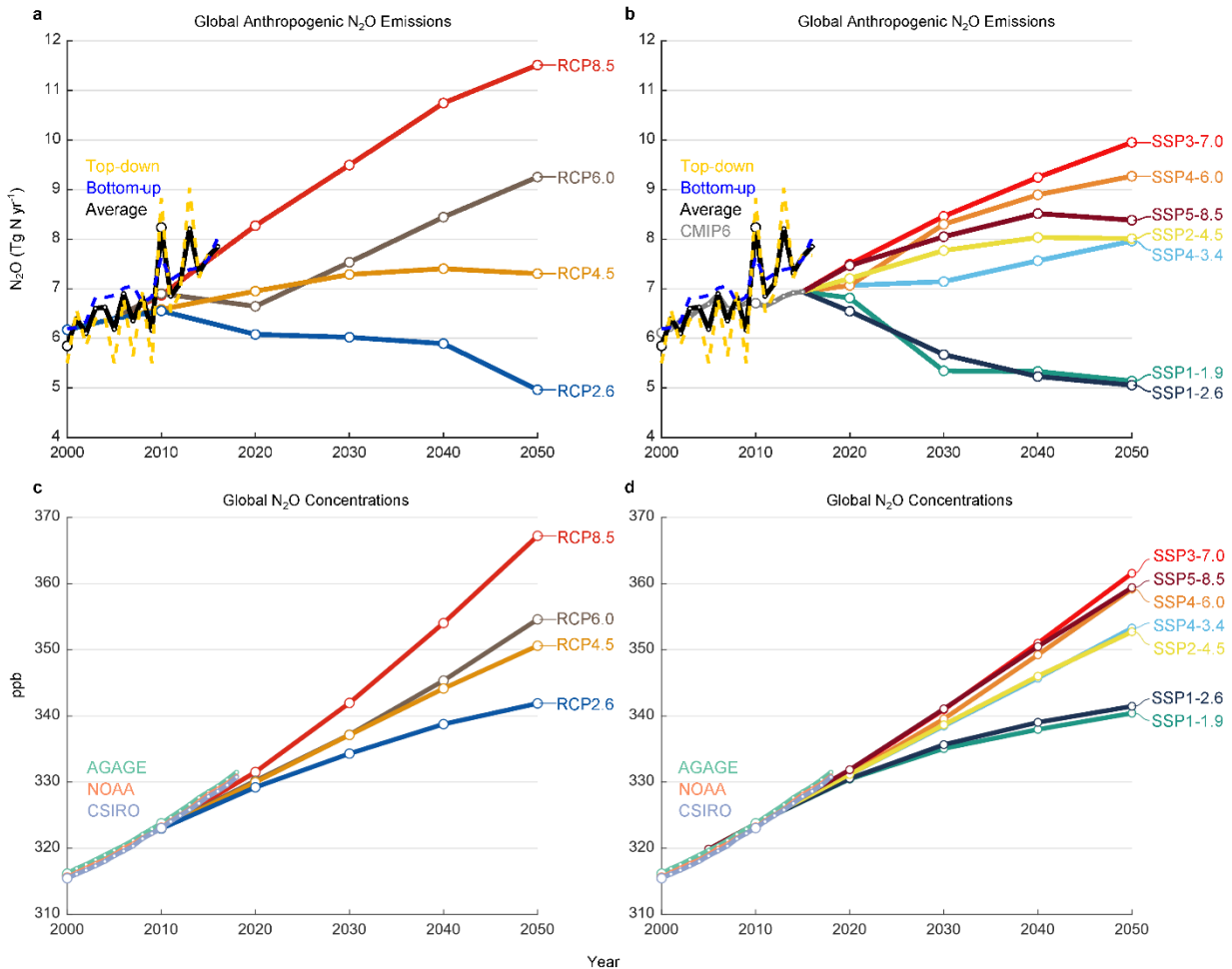
545
Fig. 4 Historical and projected global anthropogenic N₂O emissions and concentrations.
*Global anthropogenic N₂O emissions (**a, b**) and concentrations (**c, d**) compared to the four representative concentration pathways (RCPs) in the IPCC AR5 (**a**, **c**, ref. [2]) and the new marker scenarios based on the Shared Socioeconomic Pathways (SSPs) used in CMIP6 (**b**, **d**, ref. [41]). The historical data is represented as the mean of the BU and TD estimates of anthropogenic N₂O emissions, while the atmospheric concentration uses the three observation networks available, AGAGE, NOAA, and CSIRO. TD anthropogenic emissions were calculated by subtracting BU-derived natural fluxes. To aid the comparison, the four RCPs were shifted down so that the 2005 value is equal to the 2000–2009 average of the mean of TD and BU estimates. The SSPs are harmonized[3] to match the historical emissions used in CMIP6[42] and Extended Data Fig. 10 shows the unharmonized data.*

557

558

559

Methods

560

561 **Terminology.** This study provides an estimation of the global N_2O budget considering all

562 possible sources and all global change processes that can perturb the budget. A total of 18

563 sources and three sinks of N_2O are identified and grouped into six categories (Figure 1, Table 1):

564 1) Natural fluxes in absence of climate change and anthropogenic disturbances including Soil

565 emissions, Surface sink, Ocean emissions, Lightning and atmospheric production, and Natural

566 emission from inland waters, estuaries, coastal zones (inland and coastal waters), 2) Perturbed

567 fluxes from climate/CO_2/land cover change including CO_2 effect, Climate effect, Post-

568 deforestation pulse effect, and Long-term effect of reduced mature forest area, 3) Direct

569 emissions of N additions in the agricultural sector (Agriculture) including emissions from direct

570 application of synthetic N fertilizers and manure (henceforth Direct soil emissions), Manure left

571 on pasture, Manure management, and Aquaculture, 4) Indirect emissions from anthropogenic N

572 additions including atmospheric N deposition (NDEP) on land, atmospheric NDEP on ocean, and

573 effects of anthropogenic loads of reactive N in inland waters, estuaries, coastal zones, 5) Other

574 direct anthropogenic sources including Fossil fuel and industry, Waste and waste water, and

575 Biomass burning, and 6) Two estimates of stratospheric sinks obtained from atmospheric

576 chemistry transport models and observations, and one tropospheric sink (Table 1, Extended Data

577 Fig. 2).

578 For the purpose of compiling national GHG inventories for country reporting to the climate

579 convention, our anthropogenic N_2O emission categories are aligned with those used in UNFCCC

580 reporting and IPCC 2006 methodologies (Supplementary Table 14). We also provide the detailed

581 comparison of our methodology and quantification with the IPCC AR5 (see Supplementary

582 Section 4; Supplementary Table 15).

23

583   **Data synthesis.** We consider global N_2O emission from land and ocean consisting of natural

584   fluxes and anthropogenic emissions based on BU and TD approaches, however, the TD approach

585   cannot separate natural and anthropogenic sources.

586   'Natural soil baseline' emissions were obtained from six terrestrial biosphere models

587   (NMIP[16], Supplementary Tables 16−17) and provided here reflect a situation without

588   consideration of land use change (e.g., deforestation) and without consideration of indirect

589   anthropogenic effects via global change (i.e., climate, elevated CO_2, and atmospheric N

590   deposition). BU oceanic N_2O emissions were based on an inter-comparison of five global ocean

591   biogeochemistry models (Supplementary Table 18). The natural emission from 'Inland water,

592   estuaries, coastal zones' includes coastal upwelling[50] and inland and coastal waters that were

593   obtained from Yao et al.[36], Maavara et al.[35], and Lauerwald et al.[51]. Since the data (rivers,

594   reservoirs, and estuaries) provided by Maavara et al. and Lauerwald et al. are for the year 2000,

595   we assume that these values are constant during 1980−2016. Yao et al.[36] provided annual

596   riverine N_2O emissions using DLEM during the same period. Here, we averaged estimates from

597   Yao et al. with that from Maavara et al.[35]. In addition, we estimated N_2O emissions from global

598   and regional reservoirs in the 2000s, and averaged their estimates with that from Maavara et al.[35]

599   to represent emissions from reservoirs during 1980−2016. The estimate for global and regional

600   estuaries and lakes is still based on the long-term averaged values provided by Maavara et al.[35]

601   and Lauerwald et al.[51], respectively. We considered the riverine emissions in the year 1900 as

602   equivalent to the natural emission for the DLEM estimate assuming that the N load from land

603   was negligible in that period[52]. We quantified the contribution of natural sources to total

604   emission from reservoirs, lakes, and estuaries at 44% (36%−52%), with consideration of all N

605   inputs (i.e., inorganic, organic, dissolved, particulate forms). We combined the estimate from

606   lightning with that from atmospheric production into an integrated category 'Lightning and

607   atmospheric production'. We make the simplification of considering the category 'Lightning and

608   atmospheric production' as purely natural, however, atmospheric production is affected to some

609   extent by anthropogenic activities through enhancing the concentrations of the reactive species

610   NH_2 and NO_2. This category is in any case very small and the anthropogenic enhancement effect

611   is uncertain. Lightning produces NO_x, the median estimate of which is 5 Tg N yr^{-1} (ref. [53]). We

612   assumed an EF of 1% (ref. [54]) and a global estimate of 0.05 (0.02–0.09) Tg N yr^{-1} from lightning.

613   Atmospheric production of N_2O results from the reaction of NH_2 with NO_2 (refs. [55,56]), N with

614   NO_2, and oxidation of N_2 by $O(^1D)$[57], all of which constitute an estimated source of 0.3 (0.2–1.1)

615   Tg N yr^{-1}. The estimate of 'Surface sink' was obtained from Schlesinger[58] and Syakila et al.[59]

616   The anthropogenic sources include four sub-sectors:

617   **(a) Agriculture.** It consists of four components: 'Direct soil emissions', 'Manure left on

618   pasture', 'Manure management', and 'Aquaculture'. Data for 'Direct soil emissions' were

619   obtained as the ensemble mean of N_2O emissions from an average of three inventories (EDGAR

620   v4.3.2, FAOSTAT, and GAINS), the SRNM/DLEM models, and the NMIP/DLEM models. The

621   statistical model SRNM only covers cropland N_2O emissions, the same as the NMIP. Thus, we

622   add the DLEM-based estimate of pasture N_2O emissions into the two estimates in cropland to

623   represent direct agricultural soil emissions (i.e., SRNM/DLEM or NMIP/DLEM). The 'Manure

624   left on pasture' and 'Manure management' emissions are the ensemble mean of EDGAR v4.3.2,

625   FAOSTAT, and GAINS databases. Global N flows (i.e., fish feed intake, fish harvest, and waste)

626   in freshwater and marine aquaculture were obtained from Beusen et al.[30] and Bouwman et al.[60,61]

627   based on a nutrient budget model for the period 1980–2016. We then calculated global

628   aquaculture N_2O emissions through considering 1.8% loss of N waste in aquaculture, the same

629 EF used in Hu et al.[62] and Macleod et al.[31]. The uncertainty range of the EF is from 0.5% (ref. [14])

630 to 5% (ref. [63]), the same range used in the UNEP report[9]. The 'Aquaculture' emission for the

631 period 2007−2016 was a synthesis data from Hu et al.[62] in 2009, the FAO Report[31] in 2013, and

632 our calculations. The estimate of aquaculture N_2O emission prior to 2009 was from our

633 calculations only.

634   The estimated direct emissions from agriculture have increased from 2.6 (1.8−4.1) Tg N yr^{-1}

635 in the 1980s to 3.8 (2.5−5.8) Tg N yr^{-1} over the recent decade (2007−2016, Table 1).

636 Specifically, direct soil emission from the application of fertilizers is the major source and

637 increased at a rate of 0.27±0.01 Tg N yr^{-1} per decade (P < 0.05; Table 1). Compared with the

638 three global inventories (FAOSTAT, EDGAR v4.3.2, and GAINS), the estimates from process-

639 based models (NMIP/DLEM[15,16]) and a statistical model (SRNM)/DLEM[15,17] exhibited a faster

640 increase (Extended Data Fig. 4a). Over the past four decades, we also found a small but

641 significant increase in emissions from livestock manure (i.e., manure left on pasture and manure

642 management) at a rate of 0.1±0.01 Tg N yr^{-1} per decade (P < 0.05; Extended Data Fig. 4b-c).

643 Meanwhile, global aquaculture N_2O emissions increased 10-fold, however, this flux remains the

644 smallest term in the global budget (Extended Data Fig. 4d).

645 **(b) Other direct anthropogenic sources.** It includes 'Fossil fuel and industry', 'Waste and

646 waste water', and 'Biomass burning'. Both 'Fossil fuel and industry' and 'Waste and waste

647 water' are the ensemble means of EDGAR v4.3.2 and GAINS databases. The 'Biomass burning'

648 emission is the ensemble mean of FAOSTAT, DLEM, and GFED4s databases.

649   Emissions from a combination of fossil fuel and industry, waste and waste water, and biomass

650 burning increased from 1.8 (1.6−2.1) Tg N yr^{-1} in the 1980s to 1.9 (1.6−2.3) Tg N yr^{-1} over the

651 period of 2007−2016 (Table 1). The waste and waste water emission showed a continuous

652 increase at a rate of 0.04±0.01 Tg N yr^{-1} per decade (P < 0.05) (Extended Data Fig. 5c).

653 Emissions from biomass burning, estimated based on three data sources (DLEM, GFED4s, and

654 FAOSTAT), slightly decreased at a rate of -0.03±0.04 Tg N yr^{-1} per decade (P = 0.3) since

655 the1980s (Extended Data Fig. 5d). This item is largely affected by climate and land use

656 change[64,65]. Of the three data sources, the DLEM estimate exhibited significant inter-annual

657 variability, especially during 1980–2000 when extreme fire events were detected in 1982, 1987,

658 1991, 1994, and 1998. The occurrences of these extreme fires were associated with El Niño-

659 Southern Oscillation (ENSO) events, especially in Indonesia (e.g., 'Great Fire of Borneo' in

660 1982) [66]. Since 1997, N_2O emissions from fires estimated by DLEM, GFED4s, and FAOSTAT

661 were consistent in the inter-annual variability. All the three estimates showed a decreasing trend,

662 agreeing well with satellite-observed decrease of global burned area[64,65].

663 **(c) Indirect emissions from anthropogenic N additions.** Data were obtained from various

664 sources and considered N deposition on land and ocean ('N deposition on land' and 'N

665 deposition on ocean'), as well as the N leaching and runoff from upstream ('Inland and coastal

666 waters'). The emission from 'N deposition on ocean' was provided by Suntharalingam et al.[67],

667 while emission from 'N deposition on land' was the ensemble mean of an average of three

668 inventories: FAOSTAT/EDGAR v4.3.2, GAINS/EDGAR v4.3.2, and NMIP. FAOSTAT and

669 GAINS documented the sector 'Indirect agricultural N_2O emissions' by separating estimates

670 from N leaching or N deposition, while EDGAR v4.3.2 did not. Here, we treated 'Indirect

671 agricultural N_2O emissions' from EDGAR v4.3.2 as 'Inland and coastal waters' emissions for

672 data synthesis. Only EDGAR v4.3.2 provided an estimate of indirect emission from non-

673 agricultural sectors, while both FAOSTAT and GAINS, following the IPCC guidelines, provided

674 NH_x/NO_y volatilization from agricultural sectors. Here, we sum FAOSTAT or GAINS with

675 EDGAR v4.3.2 (i.e., FAOSTAT/EDGAR v4.3.2 or GAINS/EDGAR v4.3.2) to represent N

676 deposition induced soil emissions from both agricultural and non-agricultural sectors. The N_2O

677 emissions from 'Inland and coastal waters' consist of rivers, reservoirs, lakes, estuaries, and

678 coastal zone, which is the ensemble mean of an average of three inventories (EDGAR v4.3.2,

679 FAOSTAT, GAINS), and the mean of process-based models. The anthropogenic emission

680 estimated by Yao et al.[36] considered annual N inputs and other environmental factors (i.e.,

681 climate, elevated CO_2, and land cover change). For long-term average in rivers, reservoirs,

682 estuaries and lakes, we applied a mean of 56% (based on the ratio of anthropogenic to total N

683 additions from land) to calculate anthropogenic emissions. Seagrass, mangrove, saltmarsh and

684 intertidal N_2O emissions were undated from Murray et al[68]. Coastal waters with low disturbance

685 generally either have low N_2O emissions or act as a sink for N_2O[69,70]. Here, coastal zone

686 emissions were treated as anthropogenic emissions due to intensive human disturbances[71].

687   N_2O emissions following transport of anthropogenic N additions via atmosphere and water

688 bodies increased from 1.1 (0.6−1.9) Tg N yr^{-1} in the 1980s to 1.3 (0.7−2.2) Tg N yr^{-1} during

689 2007−2016 (Table 1). The N_2O emissions from inland and coastal waters increased at a rate of

690 0.03±0.00 Tg N yr^{-1} per decade ($P < 0.05$). Such an increase was reported by all the three

691 inventories (FAOSTAT, GAINS, and EDGAR v4.3.2) with FAOSTAT giving the largest

692 estimate. In contrast, the DLEM-based estimate presented a divergent trend: first increasing from

693 1980−1998 and then slightly decreasing thereafter (Extended Data Fig. 6a). Emissions from

694 atmospheric N deposition on oceans were relatively constant with a value of 0.1 (0.1−0.2) Tg N

695 yr^{-1}, while a large increase in emissions was found from atmospheric N deposition on land, with

696 0.06±0.01 Tg N yr^{-1} per decade ($P < 0.05$) reported in the three estimates (FAOSTAT/EDGAR

697 v4.3.2, GAINS/EDGAR v4.3.2, and NMIP). The FAOSTAT agricultural source, together with

28

698   the EDGAR v4.3.2 industrial source, is consistent with NMIP estimates in the magnitude of N_2O

699   emissions, with the latter estimating a slightly slower increase from 2010 to 2016 (Extended

700   Data Fig. 6b).

701   **(d) Perturbed fluxes from climate/CO₂/land cover change.** Perturbed N_2O fluxes represent the

702   sum of the effects of climate, elevated atmospheric CO_2, and land cover change. The estimate of

703   climate and CO_2 effects on emissions was based on NMIP. The effect of land cover change on

704   N_2O dynamics includes the reduction due to 'Long-term effect of reduced mature forest area'

705   and the emissions due to 'Post-deforestation pulse effect'. The two estimates were based on the

706   book-keeping approach and the DLEM model simulation. The book-keeping method is

707   developed by Houghton et al.[72] for accounting for carbon flows due to land use. In this study, an

708   observation dataset consisting of 18 tropical sites was collected to follow the book-keeping logic.

709   The dataset covers N_2O emissions from a reference mature forest and their nearby converted

710   pastures aged between one and 60 years. The average tropical forest N_2O emission rate of 1.974

711   kg N_2O-N ha^{-1} yr^{-1} was adopted as the baseline[73]. Two logarithmic response curves of soil N_2O

712   emissions (normalized to the baseline) after deforestation were developed: $y = -0.31 \ln(x) +$

713   1.53 ($R^2 = 0.30$) and $y = -0.454 \ln(x) + 2.21$ ($R^2 = 0.09$). The first logarithmic function

714   uses data collected by a review analysis[74], based upon which the second one further considers

715   observations from Verchot et al.[21] and Keller and Reiners[75]. In the first function, x (unit: year)

716   indicates pasture age in years after deforestation and y (unitless; 0–1) indicates the ratio of

717   pasture N_2O emission over the N_2O emission from the nearby reference mature forest. In the

718   second function, x (unit: year) indicates secondary forest age and y (unitless; 0–1) indicates the

719   ratio of secondary forest N_2O emission over that of a reference mature forest. This form of the

720   response functions can effectively reproduce the short-lived increase in soil N_2O emissions after

721　initial forest clearing and the gradually declining emission rates of converted crops/pastures[21,76].

722　Using these two curves and the baseline, we kept track of the N_2O reduction of tropical forests

723　and the post-deforestation crop/pasture N_2O emissions at an annual time-scale. This book-

724　keeping method was applied to the two deforestation area datasets (Supplementary Text 2.8), so

725　we could investigate not only the difference caused by the two sets of land use data but also the

726　difference between this empirical method and the process-based model. For land conversion

727　from natural vegetation to croplands or pastures, DLEM uses a similar strategy to Houghton et

728　al.[72] and McGuire et al.[77] to simulate its influences on carbon and N cycles. Moreover, through

729　using the sites of field observation from Davidson et al.[20] and Keller and Reiners[75], we estimated

730　N_2O emission from secondary tropical forests based on the algorithm: $y = 0.0084x + 0.2401$ (R^2

731　$= 0.44$). x (unit: year) indicates secondary forest age and y (unitless; 0–1) indicates the ratio of

732　secondary forest N_2O emission over that of a reference mature forest. The difference between

733　primary forests and secondary forests were subtracted from natural soil emissions simulated by

734　six terrestrial biosphere models in NMIP.

735　　　We calculated the ensemble of oceanic N_2O emission based on the BU approach (five ocean

736　biogeochemical models; Supplementary Table 18) and the TD approach (five estimates from

737　four inversion models; Supplementary Table 19), respectively. The atmospheric burden and its

738　rate of change during 1980–2016 were derived from mean maritime surface mixing ratios of

739　N_2O (refs. [78,79]) with a conversion factor of 4.79 Tg N/ppb (ref. [80]). Combining uncertainties in

740　measuring the mean surface mixing ratios[78] and that of converting surface mixing ratios to a

741　global mean abundance[80], we estimate a ±1.4% uncertainty in the burden. Annual change in

742　atmospheric abundance is calculated from the combined NOAA and AGAGE record of surface

743　N_2O and uncertainty is taken from the IPCC AR5 (ref. [2]). There shows an agreement of the

744   stratospheric loss from atmospheric chemistry transport models (TD modeled chemical sink[18,81])

745   and from satellite observations with a photolysis model (observed photochemical sink[1]), which

746   differ only by ~1 Tg N yr^{-1}. The satellite-based lifetime, 116±9 years, gives an overall

747   uncertainty in the annual loss of ±8%. The tropospheric loss of N_2O from reaction with $O(^1D)$ is

748   included in observed atmospheric chemical sink (Table 1) and is small (~1% of the stratospheric

749   sink) with an estimated range of 0.1 to 0.2 Tg N yr^{-1}.

750   **Comparison with the IPCC guidelines**. The IPCC has provided guidance to quantify N_2O

751   emissions, which is widely used in emission inventories for reporting to the UNFCCC. Over time

752   the recommended approaches have changed, which is critical for estimating emissions from

753   agricultural soils, the largest emission source. Previous global N_2O assessments[52,82,83] based on

754   the IPCC 1996 guidelines[84] attributed about 6.3 Tg N yr^{-1} to the agricultural sector, including

755   both direct and indirect emissions. This estimate is significantly larger than our results (Fig. 1;

756   Table 1) derived from multiple methods, and is also larger than the most recent estimates from

757   global inventories (EDGAR v4.3.2, FAOSTAT, and GAINS) that are based on the IPCC 2006

758   guidelines[14]. The main reason is that indirect emissions from leaching and groundwater were

759   overestimated in previous studies[85]. Correspondingly, projections of atmospheric N_2O

760   concentrations based on these overestimated emissions[82] led to biased estimates. For example,

761   Mosier and Kroeze[82] expected atmospheric N_2O concentrations to be 340–350 ppb in the year

762   2020, instead of 333 ppb[5] as observed. Recently, the 2019 Refinement to the 2006 IPCC

763   Guidelines for National Greenhouse Gas Inventories has been published. It adopts the same

764   approach for N application on soils, but considers impacts of different climate regimes. The new

765   guidelines, based on a wealth of new scientific literature, proposed much smaller emissions from

766   grazing animals by a factor of 5–7. Preliminary calculations we have made indicate that global

767   soil emissions based on these new guidelines may decrease by 20%–25%. Integrating estimates

768   relying on the IPCC methodology with estimates by process-based models provides for a more

769   balanced assessment in this paper. We also added information from assessments[86,87] that derived

770   agricultural emissions as the difference between atmospheric terms and other emissions like

771   combustion, industry and nature, and they gave comparable magnitudes (4.3–5.8 Tg N yr^{-1}) to

772   our bottom-up results.

773   **Uncertainty.** Current data analysis and synthesis of long-term N_2O fluxes are based on a wide

774   variety of TD and BU methods. TD approaches, consisting of four inversion frameworks[88-91],

775   provide a wide range of estimates largely due to systematic errors in the modelled atmospheric

776   transport and stratospheric loss of N_2O. In addition, the emissions from TD analyses are

777   dependent on the magnitude and distribution of the prior flux estimates to an extent that is

778   strongly determined by the number of atmospheric N_2O measurements[18]. Inversions are

779   generally not well constrained (and thus rely heavily on a priori estimates) in Africa, Southeast

780   Asia, southern South America, and over the oceans, owing to the paucity of observations in these

781   regions. The improvement of atmospheric transport models, more accurate priors, and more

782   atmospheric N_2O measurements would reduce uncertainty in further TD estimates, particularly

783   for ocean and regional emissions.

784   BU approaches are subject to uncertainties in various sources from land[16] and oceans[32]. For

785   process-based models (e.g. NMIP and ocean biogeochemical models), the uncertainty is

786   associated with differences in model configuration as well as process parameterization[16,32]. The

787   uncertainty of estimates from NMIP could be reduced in multiple ways[16]. First, the six models in

788   NMIP exhibited different spatial and temporal patterns of N_2O emissions even though they used

789   the same forcings. Although these models have considered essential biogeochemical processes in

32

790   soils (e.g., biological N fixation, nitrification/denitrification, mineralization/immobilization,

791   etc.)[92], some missing processes such as freeze-thaw cycles and ecosystem disturbances should be

792   included in terrestrial biosphere models to reduce uncertainties. Second, the quality of input

793   datasets, specifically the amount and timing of N application, and spatial and temporal changes

794   in distribution of natural vegetation and agricultural land, is critical for accurately simulating soil

795   N_2O emissions. Third, national and global N_2O flux measurement networks[17] could be used to

796   validate model performance and constrain large-scale model simulations. Data assimilation

797   techniques could be utilized to improve model accuracy.

798   Current remaining uncertainty in global ocean model estimates of N_2O emission includes the

799   contribution of N_2O flux derived from the tropical oceanic low oxygen zones (e.g., the Eastern

800   Equatorial Pacific, the northern Indian ocean) relative to the global ocean. These low oxygen

801   zones are predominantly influenced by high yield N_2O formation processes (e.g., denitrification

802   and enhanced nitrification). Regional observation-based assessments have also suggested that

803   these regions may produce more N_2O than is simulated by the models[32]. The current generation

804   of global ocean biogeochemistry models are not sufficiently accurate to represent the high N_2O

805   production processes in low-oxygen zones, and their associated variability (see refs. [34,93,94] for

806   more detail). Thus, precisely representing the local ocean circulation and associated

807   biogeochemical fluxes of these regions could further reduce the uncertainty in estimates of

808   global and regional oceanic N_2O emissions.

809   Regardless of the tier approach used, GHG inventories for agriculture suffer from high

810   uncertainty in the underlying agriculture and rural data and statistics used as input, including

811   statistics on fertilizer use, livestock manure availability, storage and applications, and nutrient,

812   crop and soils management. For instance, animal waste management is an uncertain aspect, since

33

813   much of the manure is either not used, or employed as a fuel or building material, or may be

814   discharged directly to surface water[95,96], with important repercussions for the calculated

815   emissions. Furthermore, GHG inventories using default EFs show large uncertainties at local to

816   global scales, especially for agricultural N_2O emissions, due to the poorly captured dependence

817   of EFs on spatial diversity in climate, management, and soil physical and biochemical

818   conditions[2,22]. It is well known, for example from the IPCC guidelines, that higher-tier GHG

819   inventories may provide more reasonable estimates by using the alternative EFs that are

820   disaggregated by environmental factors and management-related factors[97]. A large range of EFs

821   have been used to estimate aquaculture N_2O emissions[31,39,62,86] and long-term estimates of N

822   flows in freshwater and marine aquaculture are scarce[30]. Uncertainty also remains in several N_2O

823   sources that have not yet been fully understood or quantified. To date, robust estimates of N_2O

824   emissions from global peatland degradation are still lacking, although we have accounted for

825   N_2O emissions due to the drainage of organic soils (histosols) obtained from FAOSTAT and

826   GAINS databases[28,43]. Recent evidence shows that permafrost thawing[98] and the freeze-thaw

827   cycle[99] contribute to increasing N_2O emissions, which, however, have not been well established

828   in the current estimates of the global N_2O budget.

829   **Statistics.** Through using the Mann-Kendall test in R-3.4.4, we checked the significance of

830   trends in annual N_2O emissions from each sub-sector based on the BU approach.

831
832   **References**

833   50   Nevison, C. D., Lueker, T. J. & Weiss, R. F. Quantifying the nitrous oxide source from
834   coastal upwelling. *Global Biogeochemical Cycles* **18**, GB1018 (2004).
835   51   Lauerwald, R. *et al.* Natural lakes are a minor global source of N_2O to the atmosphere.
836   *Global Biogeochemical Cycles* **33**, 1564-1581 (2019).
837   52   Kroeze, C., Mosier, A. & Bouwman, L. Closing the global N_2O budget: a retrospective
838   analysis 1500–1994. *Global Biogeochemical Cycles* **13**, 1-8 (1999).

839   53   Schumann, U. & Huntrieser, H. The global lightning-induced nitrogen oxides source.
840   *Atmospheric Chemistry and Physics* **7**, 3823-3907 (2007).

841   54   De Klein, C. *et al.* N₂O emissions from managed soils, and CO₂ emissions from lime and
842   urea application. *IPCC Guidelines for National Greenhouse Gas Inventories, Prepared*
843   *by the National Greenhouse Gas Inventories Programme* **4**, 1-54 (2006).

844   55   Dentener, F. J. & Crutzen, P. J. A three-dimensional model of the global ammonia cycle.
845   *Journal of Atmospheric Chemistry* **19**, 331-369 (1994).

846   56   Röckmann, T., Kaiser, J., Crowley, J. N., Brenninkmeijer, C. A. & Crutzen, P. J. The
847   origin of the anomalous or "mass-independent" oxygen isotope fractionation in
848   tropospheric N₂O. *Geophysical Research Letters* **28**, 503-506 (2001).

849   57   Kaiser, J. & Röckmann, T. Absence of isotope exchange in the reaction of N₂O+O(^{1}D)
850   and the global Δ^{17}O budget of nitrous oxide. *Geophysical Research Letters* **32** (2005).

851   58   Schlesinger, W. H. An estimate of the global sink for nitrous oxide in soils. *Global*
852   *Change Biology* **19**, 2929-2931 (2013).

853   59   Syakila, A., Kroeze, C. & Slomp, C. P. Neglecting sinks for N₂O at the earth's surface:
854   does it matter? *Journal of Integrative Environmental Sciences* **7**, 79-87 (2010).

855   60   Bouwman, A. F. *et al.* Hindcasts and future projections of global inland and coastal
856   nitrogen and phosphorus loads due to finfish aquaculture. *Reviews in Fisheries Science*
857   **21**, 112-156 (2013).

858   61   Bouwman, A. F. *et al.* Global hindcasts and future projections of coastal nitrogen and
859   phosphorus loads due to shellfish and seaweed aquaculture. *Reviews in Fisheries Science*
860   **19**, 331-357 (2011).

861   62   Hu, Z., Lee, J. W., Chandran, K., Kim, S. & Khanal, S. K. Nitrous oxide (N₂O) emission
862   from aquaculture: a review. *Environmental science technology* **46**, 6470-6480 (2012).

863   63   Williams, J. & Crutzen, P. J. Nitrous oxide from aquaculture. *Nature Geoscience* **3**, 143
864   (2010).

865   64   Andela, N. *et al.* A human-driven decline in global burned area. *Science* **356**, 1356-1362
866   (2017).

867   65   Yang, J. *et al.* Spatial and temporal patterns of global burned area in response to
868   anthropogenic and environmental factors: Reconstructing global fire history for the 20th
869   and early 21st centuries. *Journal of Geophysical Research: Biogeosciences* **119**, 249-263
870   (2014).

871   66   Dennis, R. A review of fire projects in Indonesia (1982-1998). *Cifor* (1999).

872   67   Suntharalingam, P. *et al.* Quantifying the impact of anthropogenic nitrogen deposition on
873   oceanic nitrous oxide. *Geophysical Research Letters* **39**, L07605 (2012).

874   68   Murray, R. H., Erler, D. V. & Eyre, B. D. Nitrous oxide fluxes in estuarine environments:
875   response to global change. *Global Change Biology* **21**, 3219-3245 (2015).

876   69   Erler, D. V. *et al.* Applying cavity ring‐down spectroscopy for the measurement of
877   dissolved nitrous oxide concentrations and bulk nitrogen isotopic composition in aquatic
878   systems: Correcting for interferences and field application. *Limnology and*
879   *Oceanography: Methods* **13**, 391-401 (2015).

880   70   Murray, R., Erler, D., Rosentreter, J. & Eyre, B. Seasonal and spatial N₂O concentrations
881   and emissions in three tropical estuaries. *Marine Chemistry* 221, 103779 (2020).

882   71   Vernberg, F. J. & Vernberg, W. B. *The coastal zone: past, present, and future*. Univ of
883   South Carolina Press (2001).

884 72   Houghton, R. *et al.* Changes in the Carbon Content of Terrestrial Biota and Soils between
885   1860 and 1980: A Net Release of CO_2 to the Atmosphere. *Ecological monographs* **53**,
886   235-262 (1983).
887 73   Davidson, E. A. The contribution of manure and fertilizer nitrogen to atmospheric nitrous
888   oxide since 1860. *Nature Geoscience* **2**, 659-662 (2009).
889 74   van Lent, J., Hergoualc'h, K. & Verchot, L. V. Reviews and syntheses: Soil N_2O and NO
890   emissions from land use and land-use change in the tropics and subtropics: a meta-
891   analysis. *Biogeosciences* **12**, 7299-7313 (2015).
892 75   Keller, M. & Reiners, W. A. Soil-atmosphere exchange of nitrous oxide, nitric oxide, and
893   methane under secondary succession of pasture to forest in the Atlantic lowlands of Costa
894   Rica. *Global Biogeochemical Cycles* **8**, 399-409 (1994).
895 76   Melillo, J. M. *et al.* Nitrous oxide emissions from forests and pastures of various ages in
896   the Brazilian Amazon. *Journal of Geophysical Research: Atmospheres* **106**, 34179-34188
897   (2001).
898 77   McGuire, A. *et al.* Carbon balance of the terrestrial biosphere in the twentieth century:
899   Analyses of CO_2, climate and land use effects with four process-based ecosystem models.
900   *Global Biogeochemical Cycles* **15**, 183-206 (2001).
901 78   Dlugokencky, E., Steele, L., Lang, P. & Masarie, K. The growth rate and distribution of
902   atmospheric methane. *Journal of Geophysical Research: Atmospheres* **99**, 17021-17043
903   (1994).
904 79   Prather, M. *et al.* Annex II: Climate system scenario tables. *Cambridge, United Kingdom
905   and New York, NY, USA* (2013).
906 80   Prather, M. J., Holmes, C. D. & Hsu, J. Reactive greenhouse gas scenarios: Systematic
907   exploration of uncertainties and the role of atmospheric chemistry. *Geophysical Research
908   Letters* **39**, L09803 (2012).
909 81   Prather, M. J. & Hsu, J. Coupling of Nitrous Oxide and Methane by Global Atmospheric
910   Chemistry. *Science* **330**, 952-954 (2010).
911 82   Mosier, A. & Kroeze, C. Potential impact on the global atmospheric N_2O budget of the
912   increased nitrogen input required to meet future global food demands. *Chemosphere-
913   Global Change Science* **2**, 465-473 (2000).
914 83   Mosier, A. *et al.* Closing the global N_2O budget: nitrous oxide emissions through the
915   agricultural nitrogen cycle. *Nutrient cycling in Agroecosystems* **52**, 225-248 (1998).
916 84   IPCC. Revised 1996 IPCC guidelines for national greenhouse gas inventories. *Hayama,
917   Japan* (1997).
918 85   Nevison, C. in IPCC, Background Papers: IPCC Expert Meetings on Good Practice
919   Guidance and Uncertainty Management in National Greenhouse Gas Inventories. *IPCC
920   National Greenhouse Gas Inventories Programme, Technical Support Unit.* 381-397
921   (2000).
922 86   Crutzen, P. J., Mosier, A. R., Smith, K. A. & Winiwarter, W. N_2O release from agro-
923   biofuel production negates global warming reduction by replacing fossil fuels.
924   *Atmospheric Chemistry and Physics* **8**, 389-395 (2008).
925 87   Smith, K. A., Mosier, A. R., Crutzen, P. J. & Winiwarter, W. The role of N_2O derived
926   from crop-based biofuels, and from agriculture in general, in Earth's climate.
927   *Philosophical Transactions of the Royal Society of London B: Biological Sciences* **367**,
928   1169-1174 (2012).

929 88 Thompson, R. L. *et al.* Nitrous oxide emissions 1999 to 2009 from a global atmospheric
930   inversion. *Atmospheric Chemistry and Physics* **14**, 1801-1817 (2014).
931 89 Wells, K. C. *et al.* Simulation of atmospheric N_2O with GEOS-Chem and its adjoint:
932   evaluation of observational constraints. *Geoscience Model Development* **8**, 3179-3198
933   (2015).
934 90 Wilson, C., Chipperfield, M., Gloor, M. & Chevallier, F. Development of a variational
935   flux inversion system (INVICAT v1. 0) using the TOMCAT chemical transport model.
936   *Geoscientific Model Development* **7**, 2485-2500 (2014).
937 91 Patra, P. K. *et al.* Improved Chemical Tracer Simulation by MIROC4. 0-based
938   Atmospheric Chemistry-Transport Model (MIROC4-ACTM). *Sola* **14**, 91-96 (2018).
939 92 Tian, H. Q. *et al.* The Global N_2O Model Intercomparison Project. *Bulletin of the
940   American Meteorological Society* **99**, 1231-1252 (2018).
941 93 Suntharalingam, P. *et al.* Anthropogenic nitrogen inputs and impacts on oceanic N_2O
942   fluxes in the northern Indian Ocean: The need for an integrated observation and
943   modelling approach. *Deep Sea Research Part II: Topical Studies in Oceanography* **166**,
944   104-113 (2019).
945 94 Battaglia, G. & Joos, F. Marine N_2O Emissions From Nitrification and Denitrification
946   Constrained by Modern Observations and Projected in Multimillennial Global Warming
947   Simulations. *Global Biogeochemical Cycles* **32**, 92-121 (2018).
948 95 Galloway, J. *et al.* The impact of animal production systems on the nitrogen cycle. Vol.
949   1, *Island Press* (2010).
950 96 Steinfeld, H., Mooney, H. A., Schneider, F. & Neville, L. E. Livestock in a changing
951   landscape, volume 1: drivers, consequences, and responses. Vol. 1, *Island Press* (2013).
952 97 IPCC. 2019 Refinement to the 2006 IPCC Guidelines for National Greenhouse Gas
953   Inventories. *Hayama, Japan* (2019).
954 98 Elberling, B., Christiansen, H. H. & Hansen, B. U. High nitrous oxide production from
955   thawing permafrost. *Nature Geoscience* **3**, 332-335 (2010).
956 99 Wagner-Riddle, C. *et al.* Globally important nitrous oxide emissions from croplands
957   induced by freeze–thaw cycles. *Nature Geoscience* **10**, 279-283 (2017).
958 100 Suntharalingam, P. *et al.* Estimates of Oceanic Nitrous-oxide Emissions from Global
959   Biogeochemistry Models. *American Geophysical Union, Fall Meeting 2018* (2018).
960 101 Janssens-Maenhout, G. *et al.* EDGAR v4.3.2 Global Atlas of the three major greenhouse
961   gas emissions for the period 1970–2012. *Earth System Science Data* **11**, 959-1002
962   (2019).
963 102 Tubiello, F. *et al.* Estimating greenhouse gas emissions in agriculture: a manual to
964   address data requirements for developing countries. *FAO, Rome* (2015).
965 103 Van Der Werf, G. R. *et al.* Global fire emissions estimates during 1997-2016. *Earth
966   System Science Data* **9**, 697-720 (2017).
967 104 Dentener, F. Global maps of atmospheric nitrogen deposition, 1860, 1993, and 2050.
968   *Data set. Available on-line (http://daac. ornl. gov/) from Oak Ridge National Laboratory
969   Distributed Active Archive Center, Oak Ridge, TN, USA* (2006).
970 105 Riahi, K. *et al.* The Shared Socioeconomic Pathways and their energy, land use, and
971   greenhouse gas emissions implications: An overview. *Global Environmental Change* **42**,
972   153-168 (2017).
973

974 **Data availability**

975 The relevant datasets of this study are archived in the box site of International Center for Climate
976 and Global Change Research at Auburn University (https://auburn.box.com/). Source data for
977 Figs. 1–4, Table 1, Extended Figs. 1–10 and Supplementary Information are provided with the
978 paper. Additional description on data availability for atmospheric N_2O observations from
979 NOAA, AGAGE and CSIRO networks is provided in the Supplementary Information. The data
980 presented here are made available in the belief that their dissemination will lead to greater
981 understanding and new scientific insights on the global and regional N_2O budgets and changes to
982 it, and helping to reduce the uncertainties. As data are the result of initial processing to fit to the
983 purpose of this publication, typically a wealth of underlying information is with the original data
984 providers. Researchers interested to use results made available in the repository are encouraged,
985 as good practice, to take advantage of underlying information by contacting the original data
986 providers. If such a contact develops into a more intensive scientific discussion, further
987 involvement including co-authorship should be considered.

988

Code availability

990 The relevant codes of this study are archived in the box site of International Center for Climate
991 and Global Change Research at Auburn University (https://auburn.box.com/).

992

Acknowledgements

1033   **Author contributions**

1034   Author contributions. H.T., R.L.T., J.G.C. and R.B.J. designed and coordinated the study. H.T.,
1035   R.X., J.G.C., R.L.T., W.W., P.S., E.A.D., P.C., R.B.J., G.J.M., M.J.P., N.P., S.P., P.R., H.S.,
1036   F.N.T., S.Z., F.Z., B.F. and G.P. conducted data analysis, synthesis and wrote the paper. R.L.T.
1037   led atmospheric inversions teaming with M.P.C., T.M., D.B.M., P.K.P., K.C.W., and C.W.; H.T.
1038   led land biosphere modeling teaming with P.C., H.S., S.Z., A.A., F.J., J.C., S.R.S.D., A.I., W.L.,
1039   S.L., S.O., N.V., E.A.D., S.D. and W. Li; P.S. led ocean biogeochemical modeling teaming with
1040   G.B., L.B., S.B., E.T.B., F.J. and A.L.; P.R. led inland water and coastal modeling and synthesis
1041   teaming with B.D.E., G.G.L., R.L., T.M., P.A.R., H.T. and Y.Y.; A.F.B., J.W., M.M. provided
1042   data of N_2O flux in aquaculture. G.R.W. and J.Y. provided data of N_2O emissions from biomass
1043   burning. F.Z. provided cropland N_2O flux data from a statistical model and field observations.
1044   G.J.M., F.N.T. and W.W. provided N_2O inventory data. M.J.P. and D.J.R. provided data of
1045   stratospheric and tropospheric sinks. G.P.P. provided RCP and SSP scenarios data and analysis.
1046   B.H., E.D. and J.E. provided a global N_2O monitoring dataset of NOAA/ESRL GMD. R.P. and
1047   R.W. provided a global N_2O monitoring dataset of AGAGE stations. P.K. provided a global N_2O
1048   monitoring dataset of CSIRO. All coauthors reviewed and commented on the manuscript.
1049

1050   **Competing interests: The authors declare no competing interests.**

1051
1052   **Additional information**

1053
1054   **Supplementary information is available for this paper at https://**

1055
1056   **Correspondence and requests for materials should be addressed to H.T.**

1057   tianhan@auburn.edu
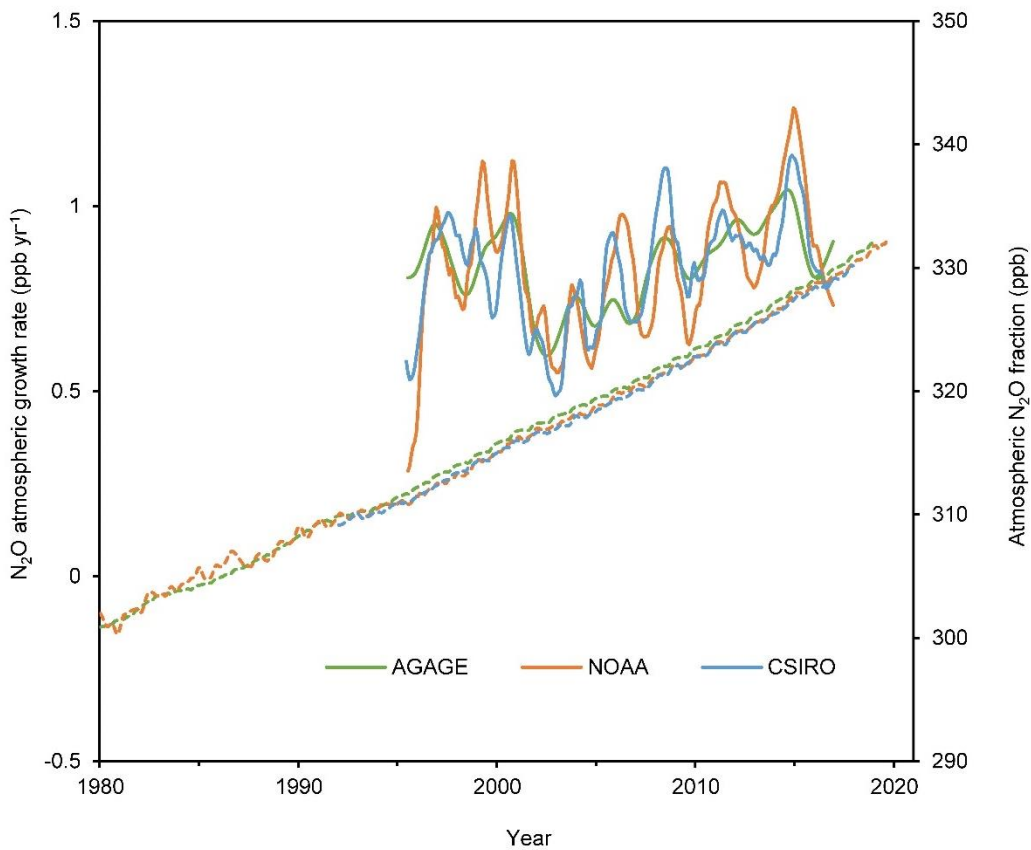
1058

Extended Data Fig. 1 Global mean growth rates and atmospheric concentration of N_2O.
Global mean growth rates (solid lines, during 1995−2017) and atmospheric N_2O concentration
(dashed lines, during 1980−2017) are from the AGAGE[6] (green), NOAA[5] (orange), and CSIRO
(blue) networks. Global mean growth rates were calculated with annual time steps and are shown
as 12-month moving averages. Growth rates are not calculated prior to 1995 due to insufficient
data and higher uncertainties on the measurements.

1059
1060
1061
1062
1063
1064
1065
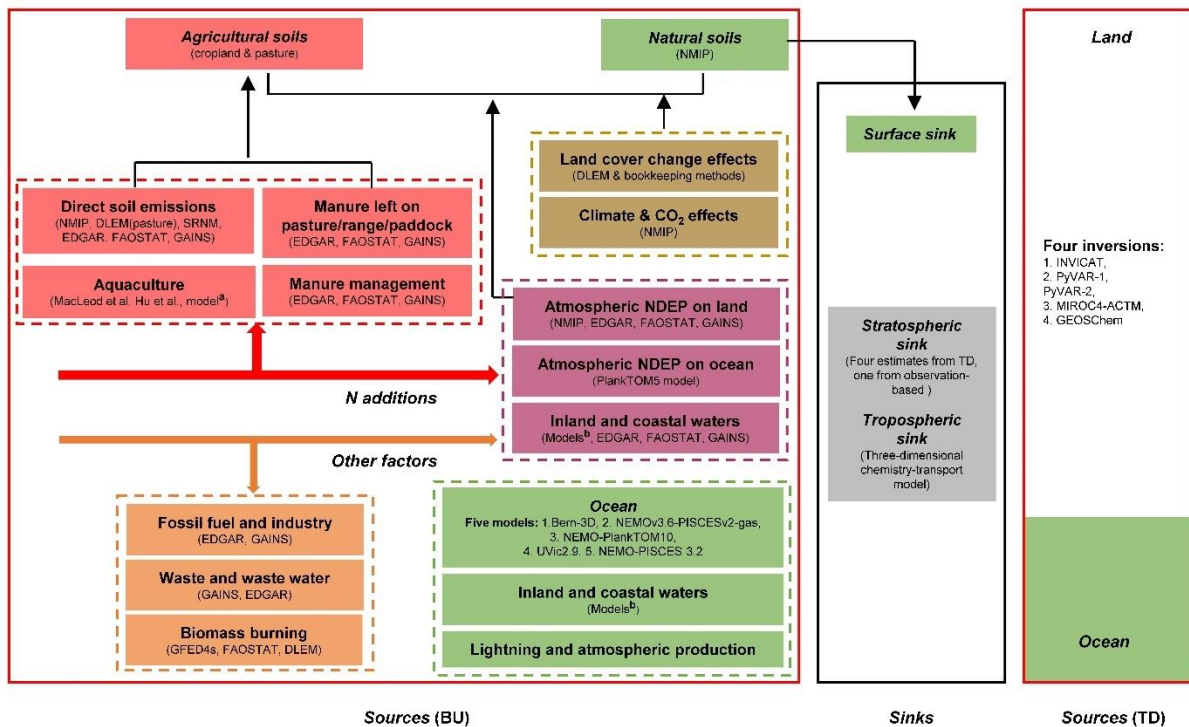
Extended Data Fig. 2 The methodology for data synthesis of global N$_2$O budget. BU and TD
represent bottom-up and top-down methods, respectively. The color codes are the same as that
used in Table 1 and Figs. 1−3. We utilize both approaches, including 22 BU and five TD
estimates of N$_2$O fluxes from land and oceans. For sources estimated by BU, we include six
process-based terrestrial biosphere modeling studies[16]; five process-based ocean biogeochemical
models[100]; one nutrient budget model[30,60,61]; five inland water modeling studies[35,36,50,51,68]; one
statistical model SRNM based on spatial extrapolation of field measurements[17]; and four GHG
inventories: EDGAR v4.3.2[101], FAOSTAT[102], GAINS[43], and GFED4s[103]. In addition, previous
literatures regarding estimates of 'Surface sink'[58,73], 'Lightning'[53,54], 'Atmospheric
production'[56,57,104], 'Aquaculture'[31,62], and model-based 'Tropospheric sink'[81] and observed
'Stratospheric sink'[1] are included in the current synthesis. [a]MacLeod et al.[31] and Hu et al.[62]
provide global aquaculture N$_2$O emissions in 2013 and in 2009, respectively; and the nutrient
budget model[30,60,61] provides N flows in global freshwater and marine aquaculture over the
period 1980−2016. [b]Model-based estimates of N$_2$O emissions from 'Inland and coastal waters'
include rivers and reservoirs[35,36], lakes[51], estuaries[35], coastal zones (i.e., seagrasses, mangroves,
saltmarsh and intertidal saltmarsh)[68], and coastal upwelling[50].
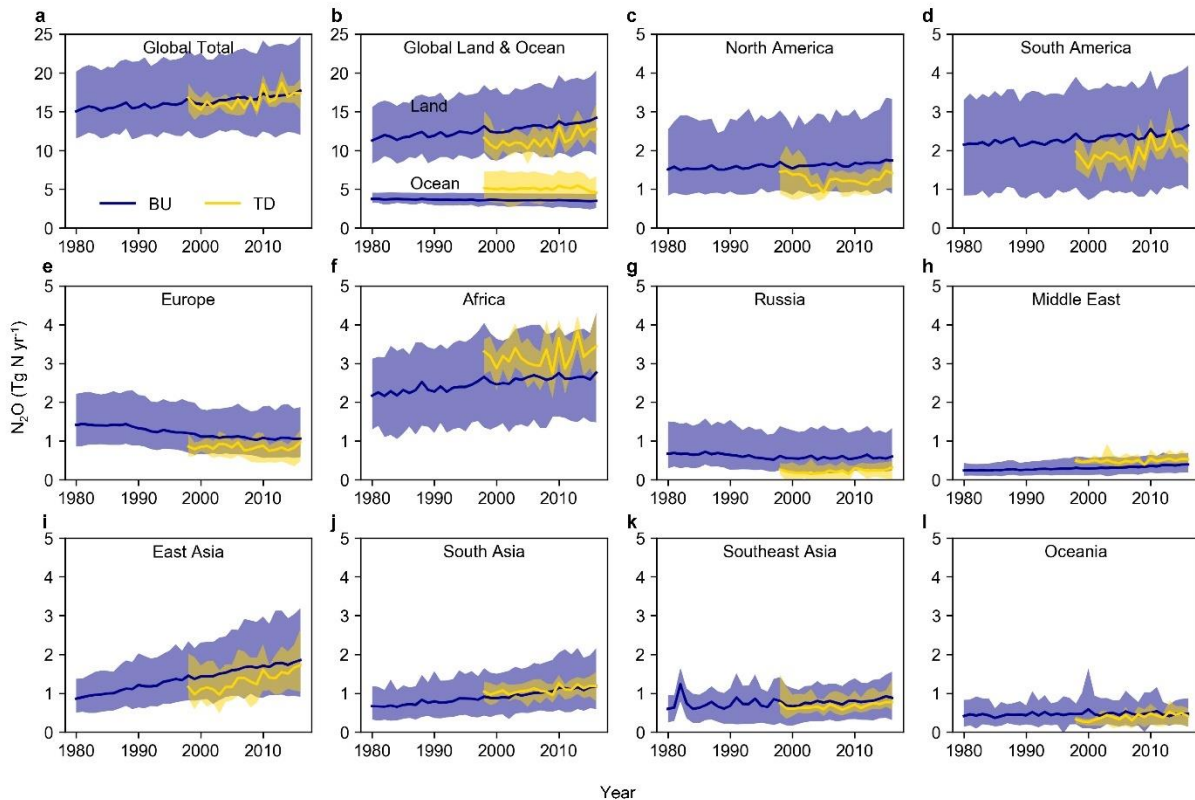
1085
**Extended Data Fig. 3 Comparison of annual total N$_2$O emissions at global and regional
scales estimated by BU and TD approaches.** The blue lines represent the mean N$_2$O emission
from BU methods and the shaded areas show minimum and maximum estimates; The gold lines
represent the mean N$_2$O emission from TD methods and the shaded areas show minimum and
maximum estimates.
1091
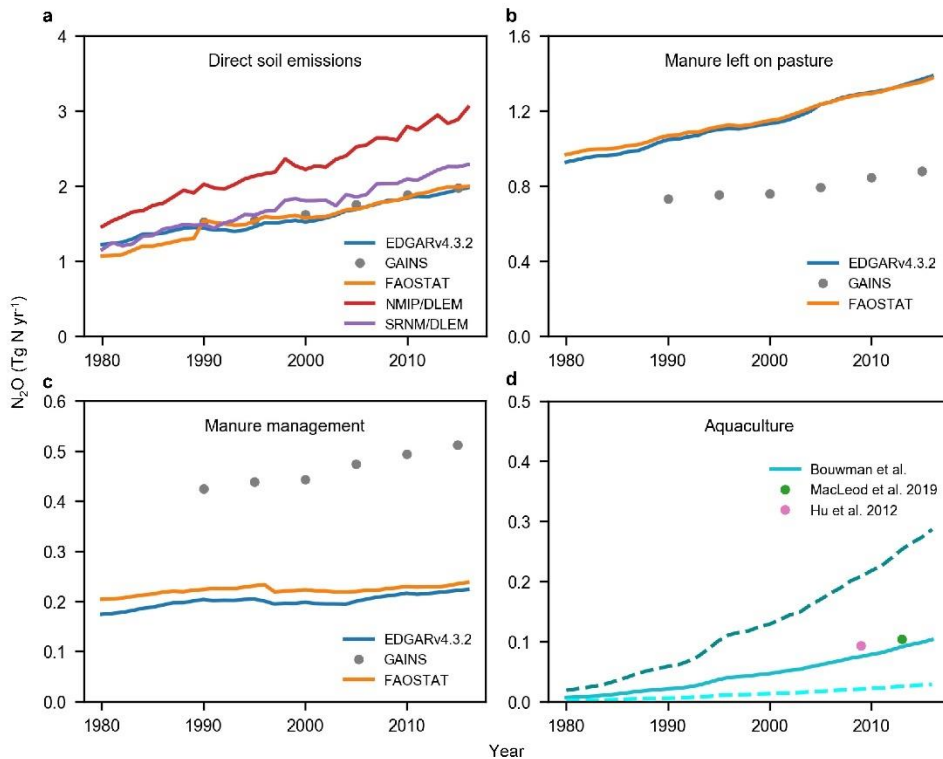
1092
1093 **Extended Data Fig. 4 Global agricultural N$_2$O emissions. a,** Direct emission from agricultural
1094 soils associated with mineral fertilizer, manure and crop residue inputs, and cultivation of
1095 organic soils based on EDGAR v4.3.2, GAINS, FAOSTAT, NMIP/DLEM, and SRNM/DLEM
1096 estimates. NMIP/DLEM or SRNM/DLEM means the combination of N$_2$O emission by NMIP or
1097 SRNM from croplands with N$_2$O emission from intensively managed grassland (pasture) by
1098 DLEM. **b,** Direct emission from the global total area under permanent meadows and pasture, due
1099 to manure N deposition (left on pasture) based on EDGAR v4.3.2, FAOSTAT, and GAINS
1100 estimates. **c,** Emission from manure management based on FAOSTAT, GAINS, and EDGAR
1101 v4.3.2. **d,** Aquaculture N$_2$O emission based on a nutrient budget model[30], MacLeod et al.[31], and
1102 Hu et al.[62]; the solid line represents the 'best estimate' that is the product of EF (1.8%) and N
1103 waste from aquaculture provided by the nutrient budget model; the dashed lines represent the
1104 minimum and maximum values.
1105
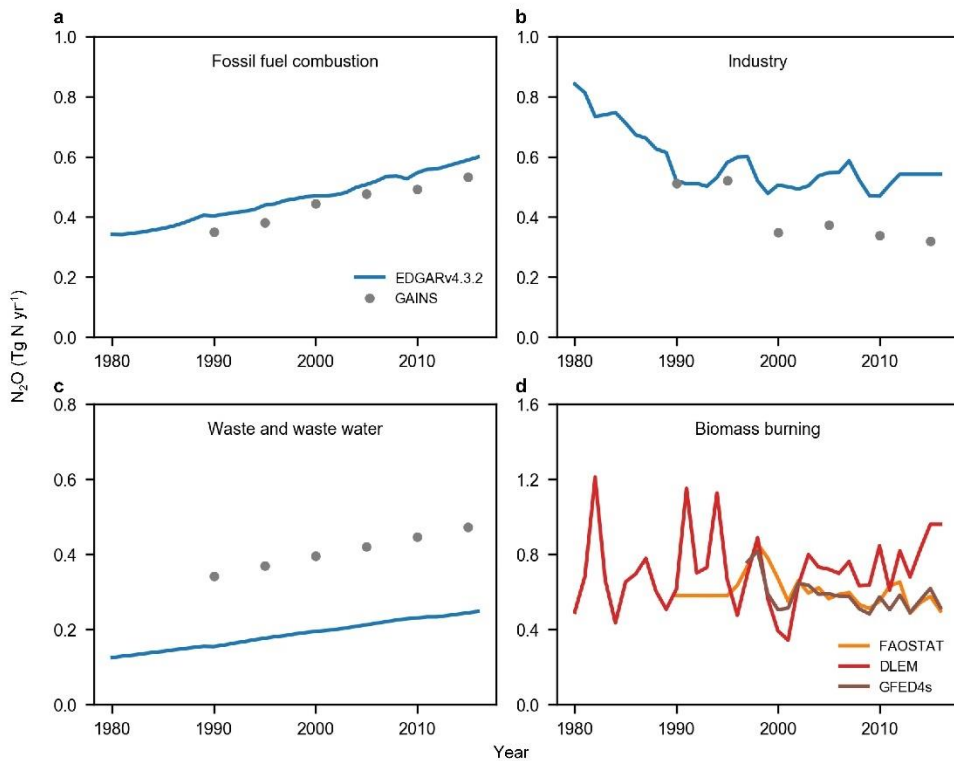
1106
1107 **Extended Data Fig. 5 Global N$_2$O emission from other direct anthropogenic sources. a,**
1108 Emission from fossil fuel combustion based on EDGAR v4.3.2 and GAINS estimates. **b,**
1109 Emission from industry based on EDGAR v4.3.2 and GAINS estimates. **c,** Emission from waste
1110 and waste water based on EDGAR v4.3.2 and GAINS estimates. **d,** Emission from biomass
1111 burning based on FAOSTAT, DLEM, and GFED4s estimates.
1112
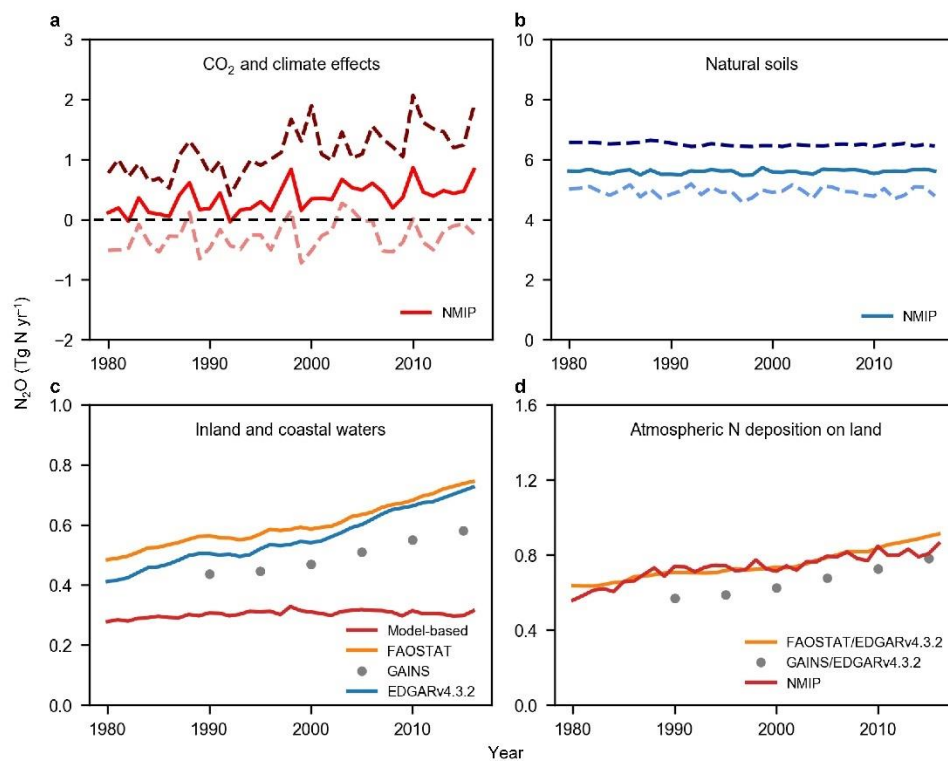
1113
Extended Data Fig. 6 Global N₂O emissions from natural soils, inland and coastal waters
and due to change in climate, atmospheric CO₂ and N deposition. a, Changes in global soil
N₂O fluxes due to changing CO₂ and climate. **b,** Global natural soil N₂O emissions without
consideration of land use change (e.g., deforestation) and without consideration of indirect
anthropogenic effects via global change (i.e., climate, elevated CO₂, and atmospheric N
deposition). The estimates are based on NMIP estimates during 1980–2016 including six
process-based land biosphere models. Here, we also subtracted the difference between with and
without consideration of secondary forests emissions that grow back after pasture or cropland
abandonment from natural soil emissions based on NMIP estimates. The solid lines represent the
ensemble and dashed lines show the minimum and maximum values. **c,** Global anthropogenic
N₂O emission from inland waters, estuaries, coastal zones based on models (model-based),
FAOSTAT, GAINS, and EDGAR v4.3.2 estimates. **d,** Emission due to atmospheric N deposition
(NDEP) on land based on NMIP, FAOSTAT/EDGAR v4.3.2, and GAINS/EDGAR v4.3.2.
FAOSTAT/EDGAR v4.3.2 or GAINS/EDGAR v4.3.2 means the combination of agricultural
source from FAOSTAT or GAINS with non-agricultural source from EDGAR v4.3.2. A process-
based model DLEM[36] and a mechanistic stochastic model[35,51] were used to estimate N₂O
emission from inland waters and estuaries, while site-level emission rates of N₂O were upscaled
to estimate global N₂O fluxes from the global seagrass area[68].

1132
1133
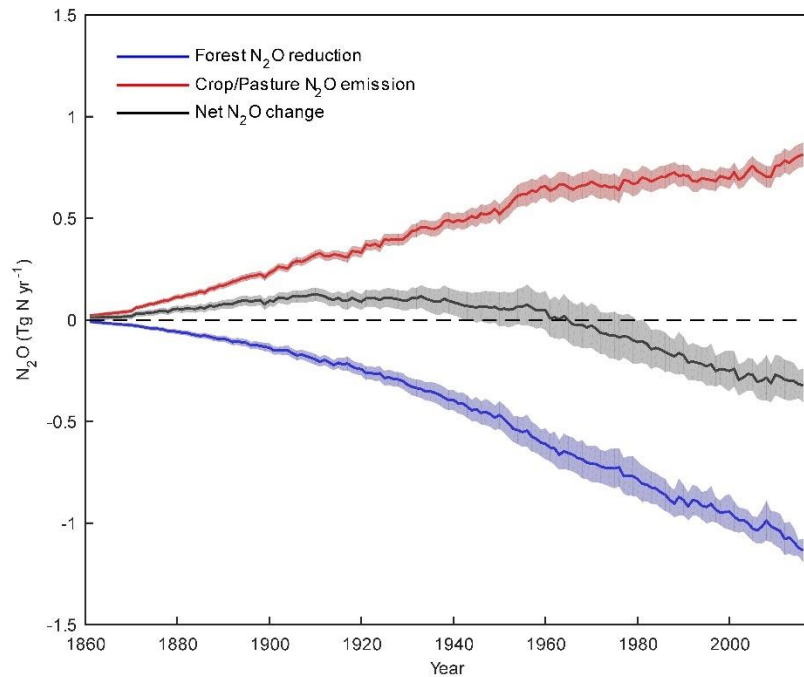
1134
1135 **Extended Data Fig. 7 Global N₂O dynamics due to land cover changes.** The blue line
1136 represents the mean forest N₂O reduction caused by the long-term effect of reduced mature forest
1137 area (i.e., deforestation) and shaded areas show minimum and maximum estimates; the red line
1138 represents the mean N₂O emission from post-deforestation pulse effect (i.e., crop/pasture N₂O
1139 emissions from legacy N of previous forest soil, not accounting for new fertilizer N added to
1140 these crop/pasture lands) and shaded areas show minimum and maximum estimates; the gray line
1141 represents the mean net deforestation emission of N₂O and shaded areas show minimum and
1142 maximum estimates.
1143
1144

a) $y = 0.56x - 1.15$, $R^2 = 0.77$

b) $y = 2.4x - 24.39$, $R^2 = 0.81$

Climate effect
Temperature (°C)
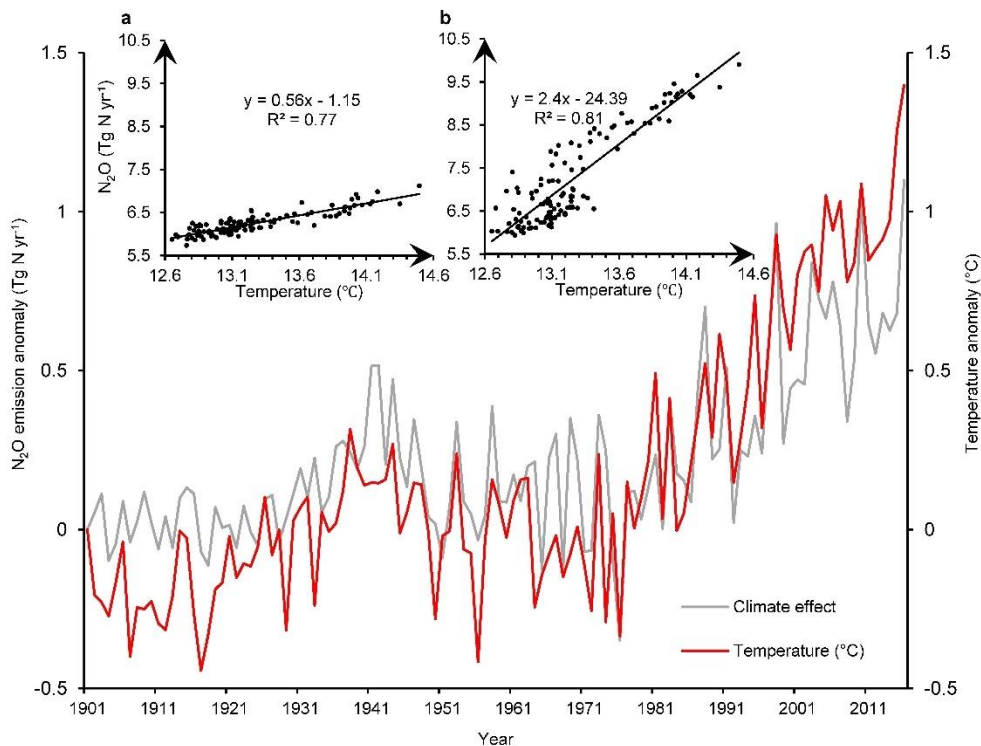
1145
1146 **Extended Data Fig. 8 Global simulated N_2O emission anomaly due to climate effect and**
1147 **global annual land surface temperature anomaly during 1901−2016.** Global N_2O emission
1148 anomalies are the ensemble of six process-based land biosphere models in NMIP. The
1149 temperature data were obtained from the CRU-NCEP v8 climate dataset
1150 (https://vesg.ipsl.upmc.fr). The above left figure **a)** shows the correlation between average global
1151 annual land surface temperature and simulated N_2O emissions (i.e., the result of SE6 experiment
1152 in NMIP[16]) considering annual changes in climate but keeping all other factors (i.e., N fertilizer,
1153 manure, NDEP, elevated CO_2, and land cover change) at the level of 1860. The above right
1154 figure **b)** shows the correlation between average global annual land surface temperature and
1155 simulated N_2O emissions (i.e., the result of SE1 experiment in NMIP[16]) considering annual
1156 changes in all factors during 1860−2016.
1157
1158
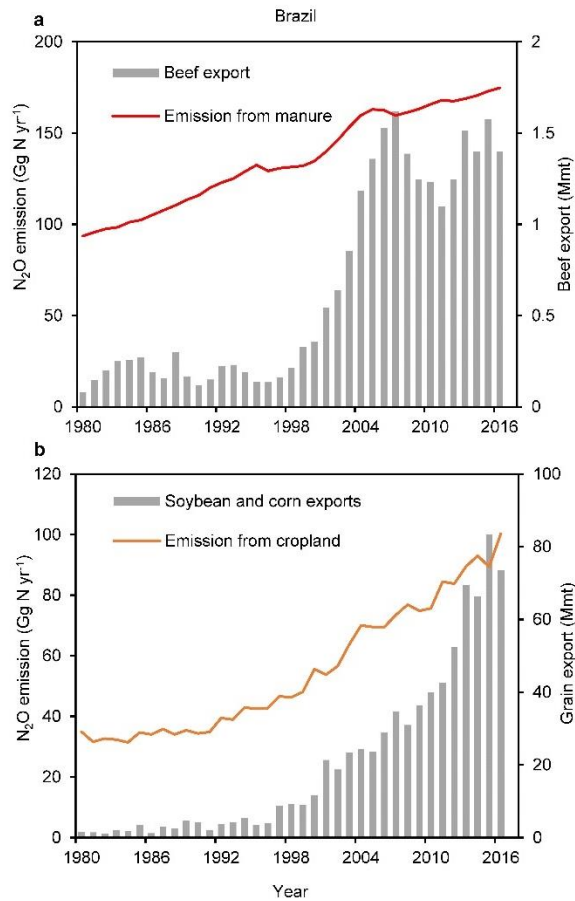
Extended Data Fig. 9 Direct soil emissions and agricultural product trades in Brazil. a, Red line shows the ensemble direct N_2O emissions from livestock manure based on EDGAR v4.3.2, GAINS, and FAOSTAT, the sum of 'manure left on pasture' and 'manure management'; The gray columns show the amount of beef export by Brazil. **b,** Orange line shows the ensemble direct N_2O emissions from croplands due to N fertilization based on NMIP and SRNM; The gray columns show the amount of soybean and corn exports by Brazil. The data of beef and cereal product trades were adapted from the ABIEC (beef) and FAOSTAT (soybean and corn). Mmt yr^{-1} represents millions of metric tons per year.

a Global Anthropogenic N₂O Emissions

b Global N₂O Concentrations
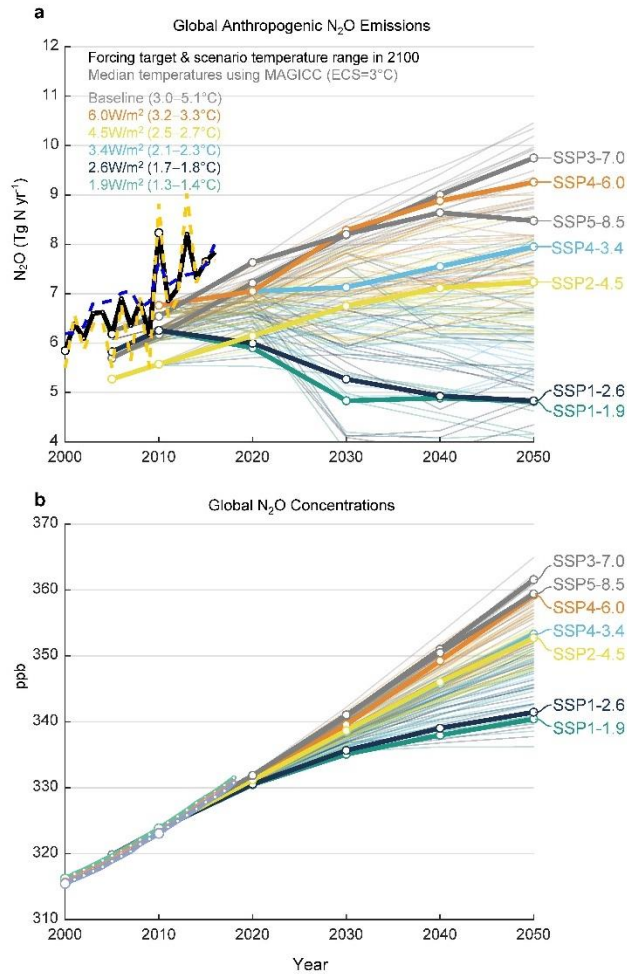
1170
1171 **Extended Data Fig. 10 An extension of Fig. 4 to provide a comparison of anthropogenic**
1172 **N$_2$O emissions (a) and atmospheric N$_2$O concentrations (b) in the unharmonized SSPs[105].**
1173 The emission and concentration data are as in Fig. 4. The unharmonized emissions from the
1174 Integrated Assessment Models (IAMs)[105] show a large variation due to different input data and
1175 model assumptions. Comparison with Fig. 4b, d illustrates the modifications to the IAM scenario
1176 data for use in CMIP6. All baseline scenarios (SSP3-7.0 and SSP5-8.5; without climate policy
1177 applied) are shown in gray regardless of the radiative forcing level they reach in 2100.